iScience

CellPress
OPEN ACCESS

Perspective

Roadmap for phase change materials in photonics and beyond

Patinharekandy Prabhathan,[1,2] Kandammathe Valiyaveedu Sreekanth,[3] Jinghua Teng,[3] Joo Hwan Ko,[4] Young Jin Yoo,[4] Hyeon-Ho Jeong,[4] Yubin Lee,[5] Shoujun Zhang,[8] Tun Cao,[9] Cosmin-Constantin Popescu,[10] Brian Mills,[10] Tian Gu,[10,11] Zhuoran Fang,[13] Rui Chen,[13] Hao Tong,[14] Yi Wang,[14] Qiang He,[14] Yitao Lu,[14] Zhiyuan Liu,[14] Han Yu,[15] Avik Mandal,[16] Yihao Cui,[16] Abbas Sheikh Ansari,[16] Viraj Bhingardive,[16] Myungkoo Kang,[17] Choon Kong Lai,[19,20] Moritz Merklein,[19,20] Maximilian J. Müller,[21] Young Min Song,[4,6,7] Zhen Tian,[8] Juejun Hu,[10,11] Maria Losurdo,[12] Arka Majumdar,[13] Xiangshui Miao,[14] Xiao Chen,[15] Behrad Gholipour,[16] Kathleen A. Richardson,[17,18] Benjamin J. Eggleton,[19,20] Matthias Wuttig,[21,22,*] and Ranjan Singh[1,2,*]

SUMMARY

Phase Change Materials (PCMs) have demonstrated tremendous potential as a platform for achieving diverse functionalities in active and reconfigurable micro-nanophotonic devices across the electromagnetic spectrum, ranging from terahertz to visible frequencies. This comprehensive roadmap reviews the material and device aspects of PCMs, and their diverse applications in active and reconfigurable micro-nanophotonic devices across the electromagnetic spectrum. It discusses various device configurations and optimization techniques, including deep learning-based metasurface design. The integration of PCMs with Photonic Integrated Circuits and advanced electric-driven PCMs are explored. PCMs hold great promise for multifunctional device development, including applications in non-volatile memory, optical data storage, photonics, energy harvesting, biomedical technology, neuromorphic computing, thermal management, and flexible electronics.

INTRODUCTION

Phase change materials (PCMs) are emerging as a versatile platform for enabling diverse functionalities in active and reconfigurable nanophotonic devices. PCMs offer stable and energy-efficient means of tuning and reconfiguring devices across a broad spectral range, from ultraviolet (UV) to terahertz (THz). Their unique and distinguishing characteristic lies in ultrafast switching speeds and a highly stable phase

[1]Division of Physics and Applied Physics, School of Physical and Mathematical Sciences, Nanyang Technological University, 21 Nanyang Link, Singapore 637371, Singapore
[2]Centre for Disruptive Photonic Technologies, The Photonic Institute, 50 Nanyang Avenue, Singapore 639798, Singapore
[3]Institute of Materials Research and Engineering (IMRE), Agency for Science, Technology and Research (A*STAR), 2 Fusionopolis Way, Innovis #08-03, Singapore 138634, Republic of Singapore
[4]School of Electrical Engineering and Computer Science, Gwangju Institute of Science and Technology, Gwangju 61005, Republic of Korea
[5]School of Materials Science and Engineering, Gwangju Institute of Science and Technology, Gwangju 61005, Republic of Korea
[6]Anti-Viral Research Center, Gwangju Institute of Science and Technology, Gwangju 61005, Republic of Korea
[7]AI Graduate School, Gwangju Institute of Science and Technology, Gwangju 61005, Republic of Korea
[8]DELL, Center for Terahertz Waves and College of Precision Instrument and Optoelectronics Engineering, Key Laboratory of Optoelectronic Information Technology (Ministry of Education of China), Tianjin University, Tianjin 300072, China
[9]DELL, School of Optoelectronic Engineering and Instrumentation Science, Dalian University of Technology, Dalian 116024, China
[10]Department of Materials Science & Engineering, Massachusetts Institute of Technology, Cambridge, MA, USA
[11]Materials Research Laboratory, Massachusetts Institute of Technology, Cambridge, MA, USA
[12]Istituto di Chimica della Materia Condensata e di Tecnologie per l'Energia, CNR-ICMATE, Corso Stati Uniti 4, 35127 Padova, Italy
[13]Department of Electrical & Computer Engineering, University of Washington, Washington, Seattle, USA
[14]Wuhan National Research Center for Optoelectronics, School of Optical and Electronic Information, Huazhong University of Science and Technology, Wuhan, China
[15]Institute of Advanced Materials, Beijing Normal University, Beijing 100875, China
[16]Nanoscale Optics Lab, ECE Department, University of Alberta, Edmonton, Canada
[17]CREOL, College of Optics and Photonics, University of Central Florida, Orlando, FL, USA
[18]Department of Materials Science and Engineering, University of Central Florida, Orlando, FL, USA
[19]Institute of Photonics and Optical Science (IPOS), School of Physics, The University of Sydney, New South Wales, NSW 2006, Australia
[20]The University of Sydney Nano Institute (Sydney Nano), The University of Sydney, New South Wales, NSW 2006, Australia
[21]Institute of Physics IA, RWTH Aachen University, 52074 Aachen, Germany
[22]Peter Grünberg Institute (PGI 10), Forschungszentrum Jülich, 52428 Jülich, Germany
*Correspondence: wuttig@physik.rwth-aachen.de (M.W.), ranjans@ntu.edu.sg (R.S.)
https://doi.org/10.1016/j.isci.2023.107946

change state that consumes zero energy. The optical and electronic properties of PCMs undergo rapid changes upon stimulation by optical and electrical pulses. These promising attributes, combined with CMOS compatibility, render PCMs suitable for an array of applications, including memory devices, tunable spatial light modulators, and flat lenses.

Progress in this field can be categorized into two primary domains. First, extensive research has been dedicated to the material aspects of PCMs, resulting in significant advancements in understanding material properties and structural transformations during phase changes. Second, various device configurations have been devised to enhance light-matter interactions and achieve tunability across different devices. Concurrently, ongoing efforts involve optimizing these devices, leveraging emerging technologies like deep learning for metasurface design and development.

Integrating PCMs with photonic integrated circuits (PICs) necessitates significant enhancements to surpass their electronic counterparts. Therefore, the forthcoming phase of research must focus on advancing energy efficiency, switching speed, and switching repeatability within these platforms.

This roadmap is structured into four key sections. It commences with an exploration of the material aspects of PCMs. Following that, it delves into the capacity to tune PCMs for photonics applications. The third section focuses on advancements in device engineering to facilitate the widespread adoption of PCMs in PICs. Finally, the fourth section spotlights advanced electric-driven PCMs capable of converting electrical energy into thermal energy.

The roadmap starts with "optical behaviour of PCMs from visible to THz" section by J.H.K. et al., explaining the optical properties of the PCMs from visible to THz frequency range. Over the broadband range, PCMs have different physical properties and corresponding different applications. There is a demand for further research and development in the field of PCMs to enhance their performance and make them suitable for various applications across the broadband range. In section "property-design of chalcogenide-based PCMs", Wuttig et al., explains material engineering aspects and property design of chalcogenide PCMs through a detailed understanding of chemical bonding and tailoring its material properties for various applications.

The significance of tunable PCMs in reconfigurable photonics applications cannot be emphasized enough. The section "tunable plasmonics with chalcogenide-based PCMs" by Prabhathan et al. explains tunable plasmonics enabled by PCMs. The conventional plasmonic materials such as gold and silver are not suitable for tuning the plasmonic resonance in the UV to visible frequency. Advanced materials and device configurations are required to meet the challenges in the UV and visible plasmonic tunability of various PCMs. In the section of "THz reconfigurable photonics with PCMs", by S.Z. et al., the authors delineate the hurdles and prospects pertaining to tunable photonics facilitated by PCMs within the THz frequency range. THz applications are in their nascent stages of development primarily because of the extended wavelengths in the THz spectrum and the substantial phase transition areas of PCMs, posing technical challenges for dynamic phase transitions. These challenges manifest in the development of THz reconfigurable devices that necessitate optical and electrical control integration. The emphasis is on surmounting current technological limitations and formulating innovative PCM compositions characterized by high index contrast, rapid response times, and minimal energy consumption.

The section "PCMs for integrated photonics" by C-C.P. et al., reflects the perspective on the key advances need to facilitate mainstream adoption of PCMs in PICs. The section "PCM antimonide sulfide devices" by M.L., solely focuses on PCM antimonide sulfide (Sb_2S_3) devices. Although there has been progress in this area, the integration of Sb_2S_3 with a commercial production line is still a challenge. The stability of the material and the development of a practical mechanism to induce the phase transition are identified as the focus of future research. Section "programmable Si photonics based on PCMs", authored by Z.F. et al., delves into the realm of programmable silicon photonics facilitated by PCMs. PCMs present an appealing prospect for achieving "set-and-forget" tuning in silicon photonics, characterized by their compact device footprint and remarkable energy efficiency. Nevertheless, certain challenges warrant attention, including enhancing endurance, attaining CMOS-level voltage control, mitigating insertion loss, augmenting the extinction ratio, enabling multilevel operation, and ensuring seamless compatibility with existing production processes. The successful resolution of these challenges could pave the way for PCMs to offer solutions for large-scale programmable gate arrays.

Section "chalcogenide photonic ICs for reconfigurable and nonlinear functionality", by C.K.L. et al., of the roadmap focuses on the status of chalcogenide PICs and the promising platforms for integrating these materials. This section recognizes that a single platform cannot fulfill the diverse requirements for various functions, including microwave sources, signal processing, non-volatile memory, and optical computing. Therefore, the focus lies in investigating the heterogeneous integration of distinct material systems to realize the desired chalcogenide PICs.

The section "ultrafast and non-volatile all-optical switch enabled by all-dielectric PCMs" by H.T. et al., discusses the status, current and future challenges in the field of ultrafast and non-volatile all-optical switch enabled by all-dielectric PCM. Advancement in the field of reconfigurable phase change photonic metasurfaces is explained and future research directions are outlined in the section "reconfigurable phase change photonic metasurfaces" by A.M. et al.

PCMs represent just one of numerous materials that must coexist alongside a variety of other materials on a planar substrate for integrated photonic applications. The summary in section "engineering multi-material solutions for PCMs-based integrated photonics" by M.K. et al., highlights key issues that must be considered when choosing suitable, often diverse material solutions, needed to realize specific optical functions.

In the last section "PCMs for electro-thermal conversion and storage" by H.Y. et al., advanced functional electric-driven phase change materials (EPCMs) that can convert electrical energy into thermal energy is presented as a significant material that plays a key role in sustainable energy utilization.

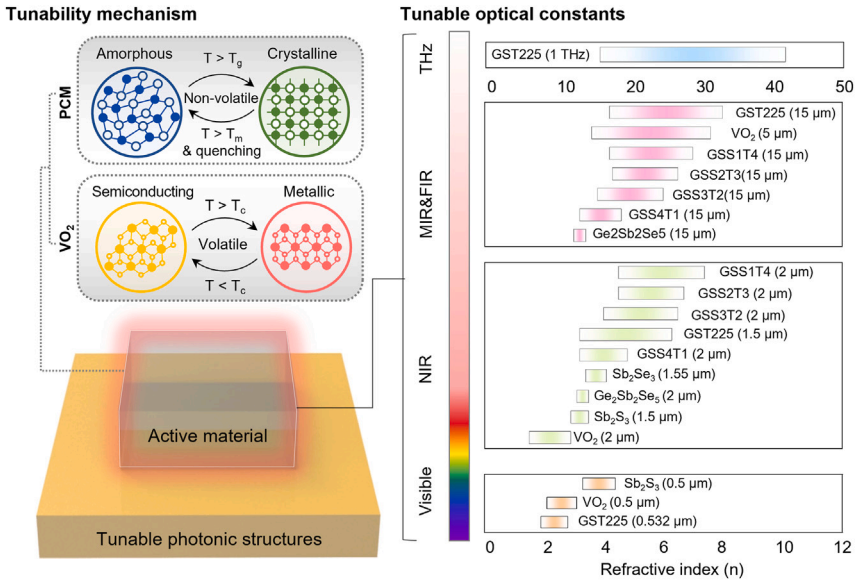

Figure 1. Refractive index variation of PCMs from visible to terahertz
The refractive indices are obtained from the literatures Adapted from.[2–12]

Optical behavior of PCMs from visible to terahertz by J.H.K., Y.J.Y., Y.L., H-H.J., Y.M.S.

PCMs are thermal energy-induced active materials, which show large optical property changes. Representatively, Ge-Sb-Te (GST) and its family materials have attracted great attention in various applications due to its non-volatile and fast/reversible phase change (i.e., between amorphous and crystalline states). The phase change is originated by the reconfiguration of atomic bonding induced by thermal energy at critical temperature ($T_c \approx 160°C$, i.e., crystallization) and melting temperature ($T_m \approx 600°C$, i.e., re-amorphization with quenching). In the case of transition metal oxides, VO_2 has been used in many applications, which shows a drastic complex refractive index change at low temperature ($T_c \approx 70°C$). Also, the composition x of $W_xV_{1-x}O_2$ determines the transition temperature (e.g., 0.015 of x shows T_c at 22°C). Also, owing to their large optical index variations and excellent CMOS compatibility, PCMs have been utilized in various fields of research (e.g., memory devices, tunable color filters, thermal emission modulator, and tunable metasurfaces). It is noteworthy that each application has different operating wavelengths, which demand appropriate optical properties (complex refractive index and its variation). Therefore, the guidelines for case-by-case designs of photonic structure upon target applications are required by suggesting alternative active materials.[1] Fortunately, a great tunability of the PCMs and various promising active materials provide an opportunity for strategic demonstration of diverse optical properties.

Over the broadband range, PCMs have different physical properties and corresponding applications, so it is essential to present several cases and accurate indices. As described in Figure 1, PCMs and phase transition materials, which include $Ge_2Sb_2Te_5$ (GST-225), $Ge_3Sb_2Te_6$ (GST-326), $Ge_2Sb_2Se_1Te_4$ (GSST-2214), $Ge_2Sb_2Se_2Te_3$ (GSST-2223), $Ge_2Sb_2Se_3Te_2$ (GSST-2232), $Ge_2Sb_2Se_4Te_1$ (GSST-2241), $Ge_2Sb_2Se_5$, Sb_2S_3, Sb_2Se_3, and VO_2, show various refractive indices and variations ranges. The extinction coefficient (k) of PCM is also considered as an important factor in many applications. For example, the extinction coefficient of GSST is varied as a Te is substituted by a lighter Se atom, which increases the band gap and reduces the excessive loss. The presence of the extinction coefficient is a crucial point since it fundamentally limits many applications, including tunable metasurfaces, optical memory devices, and optical communications. On the other hand, in some cases, non-trivial phase shift has been utilized for ultrathin colorations based on the presence of extinction coefficient.[13–15] For example, the modulation of complex refractive index shows drastic color modulation based on the phase change from amorphous to crystalline state resulting in blue-shifted color change.[16] As discussed, engineering the optical properties of active materials is necessary to apply active materials into appropriate applications in a broad range of targeted spectra.

PCMs have excellent reversibility, fast-tunability, and stability, therefore, they have been widely used in various applications such as structural coloration, metasurface, photonic memory, thermal radiation, and THz plasmonics (Figure 2). However, the innate limitation of PCMs, i.e., high-power consumption while phase change, is still a significant problem, leading to huge energy loss. Furthermore, PCMs possess large optical losses in visible and near-infrared (NIR) wavelength regimes. These two factors should be considered for designing reconfigurable optical devices. For example, GSST alloy provides advantages compared to GST such as broadband transparency (i.e., low optical loss at short wavelength range) and larger switching volume (i.e., efficient phase change over the structures), while showing great reversibility. Accordingly, recent destinations of PCMs are targeted to reach high-performance/broadband operations by developing and searching for new/advanced materials. Together with the PCMs, recent progress on diverse active materials have been accelerated for achieving photonic responses with suitable complex refractive index tuning.[23] Among them, optically active materials have shown the excellent ability in low energy consumption or transparent optical property (i.e., low extinction coefficient at shorter wavelength range). For example,

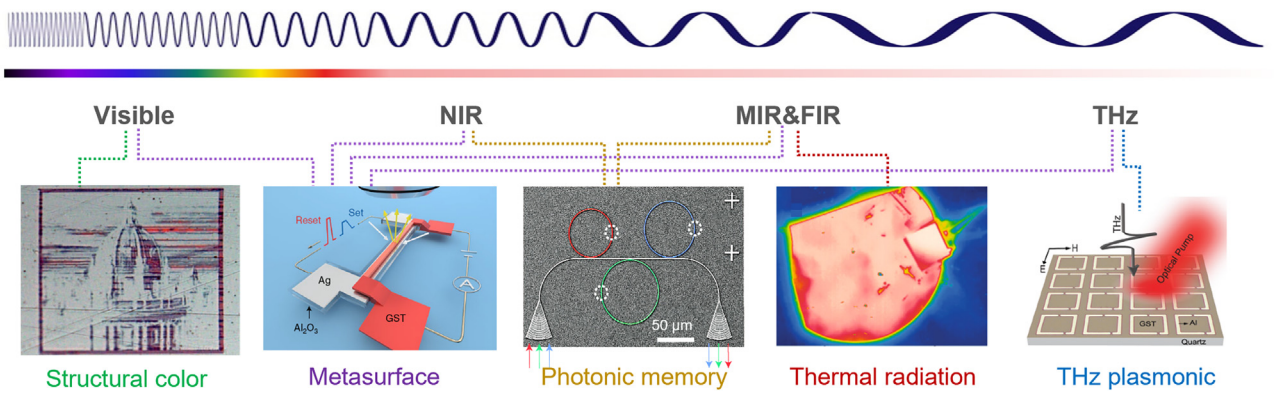

Figure 2. Applications of tunable photonics with PCMs
Reproduced with permission from.[17–22]

electrochemical modulations that cause refractive index variations in conducting polymers require relatively mild driving energy. Due to their small energy consumption, even lower than commercial e-paper, they have been presented in diverse tunable photonics, such as color display, wavefront steering, or thermal emission modulator. However, the chemical reaction of electrochemical reconfigurable photonics limits the modulation speed. Meanwhile, some cases of free-carrier pumping in dielectric or semiconductor show very fast modulation frequencies up to GHz level. However, they also have limitations of narrow modulation range and energy loss. As described in above, complementary guidelines for the material selection and development of the physical properties are important.

In conclusion, the excellent reversibility, stability, and optical properties of PCMs allow promising/high-performance technologies to successfully present applications including structural color, metasurfaces, photonic memory, thermal radiation, and THz plasmonics. Corresponding to the target wavelengths (but broad range), the optical/physical properties (e.g., complex refractive index, variation range, and modulation thickness) are varied with each active material. The rapid development of material engineering and modern physics, optically active materials, e.g., PCMs, carrier-pumping dielectric/semiconductor, electrochemical reaction induced conducting polymer, and liquid crystals, have shown remarkable abilities toward achieving practical/futuristic applications. Nevertheless, tunable photonics are in an early stage and still need to be developed to solve the limitations of material itself. To satisfy the industrial needs, such as optical loss, energy efficiency, scalability, reversibility, and modulation speed, the designation of tunable photonics should be carefully addressed according to the target applications and further technical development are necessary.[1]

Property-design of chalcogenide-based phase change materials by M.W. and M.J.M.

The application potential of PCMs has fascinated scientists and engineers for decades. One of the first people to realize this potential was S. R.O., who wrote a paper about reversible electrical switching phenomena in disordered structures already in 1968.[24] A few years later, he reported with a team of colleagues on the rapid reversible light-induced crystallization of amorphous semiconductors.[25] Both findings initiated the development of novel technologies. Electrical switching processes are now utilized in non-volatile electronic memories and threshold switches, while laser-induced reversible switching of chalcogenides is employed in rewritable optical disks. Today, there are many more potential applications, which can be realized with PCMs, i.e., materials which can be switched rapidly and reversibly between amorphous and crystalline phases. Such applications include neuromorphic computing,[26] photonic switches[27] and displays[28] to mention just a few. Given the striking range of potential applications as well as the remarkable material properties which enable those, it is surprising that there are on-going debates about the origin of these properties. In the following, we will demonstrate how a detailed understanding of chemical bonding in PCMs can help to tailor material properties for various applications of this material class.

In the last two decades, quantum-chemical tools have been developed which enable the quantification of chemical bonds in solids. This approach has recently been utilized to characterize bonding in chalcogenides like GeTe and Sb_2Te_3.[29,30] These concepts are in part based on the quantum theory of atoms in molecules (QTAIM). Using this scheme, the number of electrons transferred between adjacent atoms (more precisely their corresponding basins) can be calculated. To compare different solids and their degree of charge transfer, the number of electrons transferred by an atom is divided by the formal oxidation state. This renormalized electron transfer hence provides a quantitative measure of the degree of ionic bonding. Furthermore, the number of electron pairs formed between adjacent atoms can be determined from the corresponding delocalization index. These two quantities have been shown to span a map.[31] The result is depicted in Figure 3, where instead of the number of electron pairs formed between adjacent atoms, the number of electrons shared between adjacent atoms is given as the y axis. This map separates different bonding mechanisms rather well. Ionic bonding is characterized by pronounced electron transfer between adjacent atoms, while in covalent bonding pronounced electron sharing (electron pair formation) prevails. The large number of nearest neighbors in metals leads to a small number of electrons shared between adjacent atoms. In conjunction with moderate charge transfer this locates solids which employ metallic bonding in the lower left corner of the map. Between covalent and metallic bonding, another bonding

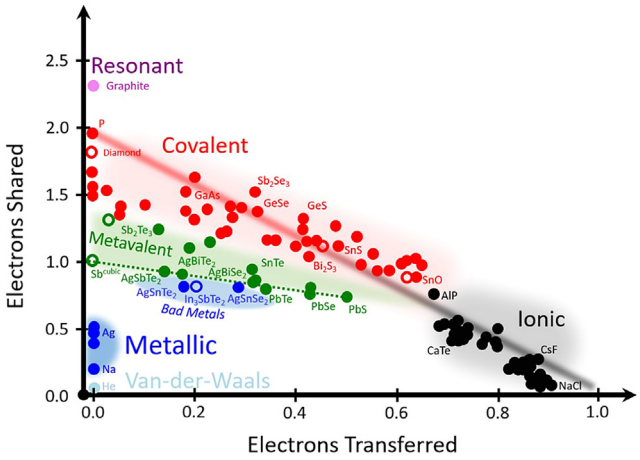

Figure 3. 2D map classifying chemical bonding in solids

The map is spanned by the number of electrons shared between adjacent atoms and the electron transfer renormalized by the formal oxidation state. Different colors characterize different material properties and have been related to different types of bonds. Adapted from.[29–31] Filled and open symbols represent thermodynamically stable and metastable phases. The red – black line describes the transition from ideal covalent bonds to perfect ionic bonds. The dashed green line indicates metavalently bonded solids with perfect octahedral arrangement like cubic Sb, $AgSbTe_2$ and PbS, while distorted octahedrally coordinated structures are situated above it, characterized by a larger number of electrons shared. Map adapted from.[32]

mechanism is located, which is characterized by a characteristic property portfolio including large values of the Born effective charge Z* and the optical dielectric constant ε_∞. Solids which are characterized by these properties have been denoted as 'metavalent' solids or incipient metals.[31] Crystalline GeTe and $GeSb_2Te_4$ fall into this category.[33,34]

Interestingly, these metavalent solids have a property portfolio which differs significantly from solids which employ ionic, covalent, or metallic bonding. This implies that metavalent bonding is indeed a fundamental and unique bonding mechanism in solids, a claim that has recently been confirmed based on property classification[35] and detailed DFT calculations.[36] Amorphous PCMs on the contrary employ ordinary covalent bonding, i.e., a 2c – 2e bonding.[37] Hence, PCMs undergo a change of bonding mechanism from metavalent to covalent bonding upon vitrification.[37] This finding helps to understand why PCMs undergo a significant change of properties upon crystallization. More importantly, the map in Figure 3 can also be employed to describe and predict property trends. This is depicted in Figure 4, where systematic changes in crystallization speed are displayed.[38,39] The crystallization speed is crucial for PCMs, since this process is the time limiting step for PCMs.[40] Hence, it is important to identify chalcogenides which crystallize rapidly.

Our findings are summarized in Figure 4, which shows the metavalently bonded solids are characterized by fast crystallization. More importantly, Figure 4 shows systematic trends. Upon increasing the number of electrons shared in the crystalline state, crystallization proceeds more slowly. Hence, fast alloys are located close to the dashed line in Figure 3, where metavalent solids with minimum distortion, i.e., perfect octahedral coordination are found. Hence, Figure 3 in conjunction with Figure 4 provides a roadmap where PCMs are located which crystallize rapidly.

While the two figures discussed here provide a new avenue to design PCMs for optical applications, Figure 4 only shows property trends for one important criterion, the crystallization speed. PCMs must meet several additional requirements including the optical contrast, a sufficiently large bandgap, good cyclability, good chemical stability and several other quantities.[41,42] All these requirements must be met. Hence, it is mandatory to find property trends like the one shown in Figure 4 also for all other relevant material properties. It will be crucial to understand and design property trends in this multidimensional space. For example, there is a strong push to develop PCMs which have pronounced contrast also for shorter wavelengths. This can be accomplished by replacing tellurides by selenides or even sulfides. Figure 4 shows that such Te-Se alloys still employ metavalent bonding, if the concentration of Se is not too high. Indeed, such compounds have a larger bandgap. Yet, they are also typically much slower in crystallization speed.[38,39] Hence, either property compromises must be identified or maps like Figures 3 and 4 need to be employed to identify sweet spots in multi-dimensional property space.

As already mentioned in the last paragraph, identifying correlations for relevant material properties is one of the most pressing needs for material scientists. Fortunately, the concepts of machine learning and property classification could help to solve this task. We are optimistic that such property correlations will be identified and understood with the tools to quantify chemical bonding discussed here. Yet, there are three other potentially promising directions that should be considered as well. In recent years, several materials have been identified which share some of the remarkable properties with PCMs. Crystalline halide perovskites, for example, also employ a bonding mechanism which closely resembles metavalent bonding.[43] This helps to explain the strong absorption and favorably low effective masses of this material class. If it would be possible to also stabilize glassy halide perovskite this could lead to PCMs which would work at much shorter wavelengths, since these halide perovskites have larger bandgaps. Furthermore, it would in general be interesting to explore the border regions of metavalent

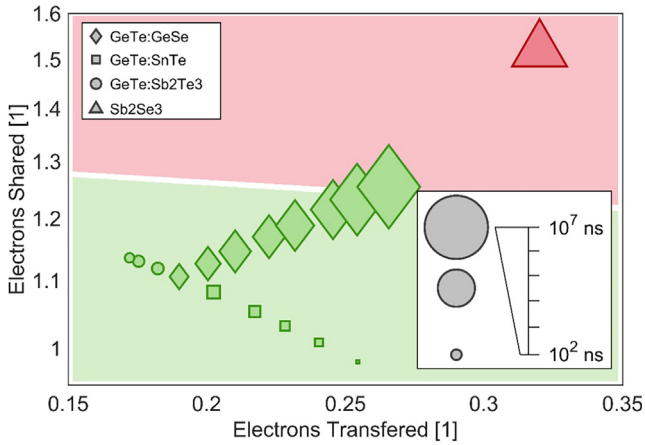

Figure 4. Minimum crystallization time and its dependence on the chemical bond indicators introduced in Figure 3

Sb_2Se_3 represents a covalently bonded material, while typical phase change materials like $Ge_2Sb_2Te_5$ or GeTe are metavalently bonded. Adapted from.[38,39]

bonding toward covalent bonding,[32] ionic bonding[44] and metallic bonding.[45] It is expected that in these border regions interesting material properties should be located.

Finally, it seems worthy to also explore how material properties change in reduced dimensions. It has recently been suggested that the properties of metavalent solids respond strongly toward confinement.[46] This implies that reducing the thickness of such chalcogenides will also modify material properties, an alternative to stoichiometry tailoring. Indeed, recent findings show that the structure and properties of thin films such as crystalline GeTe show interesting confinement effects, while no comparable effect has been found for amorphous GeTe films.[33] It will be interesting to follow systematic studies of such confinement effects in metavalent solids.

Tunable plasmonics with chalcogenide phase change materials by P.P., K.V.S., J.T., R.S.

Chalcogenide PCMs enabled optical platforms are highly promising for reconfigurable nanophotonics systems due to their large variation in optical contrast during the structural phase transition from amorphous to crystalline. Various PCMs have been widely explored in different configurations together with metals and dielectrics to tune the spectral response from UV to THz spectral bands. Among them, $Ge_2Sb_2Te_5$ (GST) and its other stoichiometric combinations are highly promising due to their fast-switching speed and low-loss at infrared (IR) to THz region. Figure 5 explains a chronological graph showing various PCM based platforms explored for tunable nanophotonic applications from UV to THz. This include PCMs such as gallium lanthanum sulfide GL,[47] $Ge_2Sb_2Te_5$ (GST) in near-IR (NIR),[48–52] GST in mid-IR (MIR) to THz,[22,53–65] GST in visible (VIS),[20,21,66] $Ge_3Sb_2Te_6$ in MIR,[67,68] $Ge_3Sb_2Te_6$ in NIR,[69] $Ge_2Sb_2Se_4Te_1$ (GSST) in MIR,[70]GSST in NIR,[71–75] GST in VIS to NIR,[76–78] bismuth telluride (Bi:Te) in the VIS,[79] Sb_2S_3 in the VIS to NIR,[80–94] Sb_2Se_3 in the VIS to NIR.[2,95,96] From Figure 5, it is evident that a substantial amount of research has been done in the NIR to THz region of the electromagnetic spectrum to demonstrate tunable nanophotonic properties using PCMs, especially on a GST platform. Nevertheless, comparatively less materials were explored in the UV-VIS region. In addition, PCMs also explored in the microwave frequencies particularly for switching applications.[97]

Tunable plasmonics by PCMs

For chip-scale reconfigurable nanophotonic systems, dynamic tuning of optical and plasmonic properties in the UV to visible frequency range are particularly important.[85,90,91,93] The conventional plasmonic materials such as gold and silver are not suitable for tuning the plasmonic resonance in this frequency band. Therefore, alternate tunable plasmonic materials with high plasmonic figure of merit (FOM) are required to meet a comparable functionality to that of a noble metal. For tunable plasmonics applications, different PCM-integrated tunable structures have been demonstrated, where PCM only works as a switching agent for metal-based plasmonics. To realize low-loss tunable plasmonic devices at UV-visible wavelengths, all-PCM plasmonic structures without a lossy metal is required. A dielectric to plasmonic transition in the UV-visible wavelength range was demonstrated by switching the structural phase of GST from amorphous to crystalline [33]. This indicates that a nanostructured thin film of GST shows plasmonic resonance only in the crystalline phase.[86,88,98] It has been reported that the different stoichiometrically engineered PCM alloys also show negative real permittivity in the amorphous phase. For example, plasmonic resonance was reported using the nanopatterned thin films of amorphous Bi:Te.[79] However, the thin film of PCMs should show negative real permittivity in both amorphous and crystalline phases for tunable plasmonics applications.

Recently, the tunable plasmonic resonance in the visible wavelength range was experimentally demonstrated using Sb_2Te_3 based subwavelength structures.[85,90,91] The plasmonic resonance of a Sb_2Te_3 based metasurface is continuously tuned using an electrical signal. Figures 6A and 6B illustrate the optical image of a fabricated microheater integrated tunable device and the scanning electron

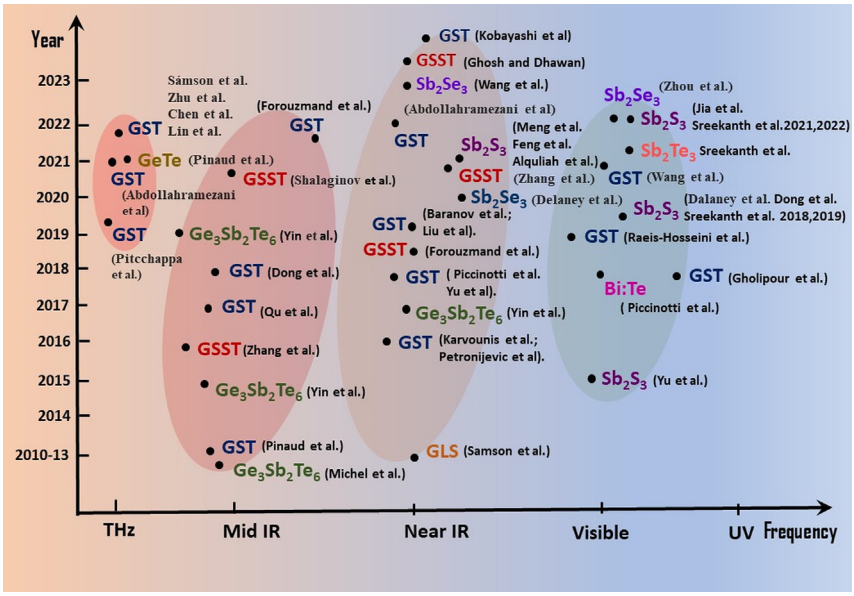

Figure 5. Various PCM platforms explored for demonstrating tunable nanophotonic applications in the UV to THz spectral range

microscope image of Sb_2Te_3 based metasurfaces, respectively. Since Sb_2Te_3 offers the fastest crystallization speed, its glass transition and melting temperature decrease, as a result it can be crystalized and re-amorphized at lower temperatures compared to GST. In Figures 6C and 6D, we show the electrical continuous tuning of plasmonic resonance of metasurface by switching the phase of Sb_2Te_3 from amorphous to crystalline. As it is shown, the continuous tuning of plasmonic resonance toward lower wavelength with increasing current (20–60 mA) was obtained. We noticed a blue shifted wavelength of ~50 nm with a DC current of 60 mA (temperature <100°C).

For light manipulation and control, a wide variety of materials are available in the NIR to visible spectral bands, providing numerous functionalities with a broadband spectral response and low loss. However, in the UV region, most of the material is characterized by narrow spectral response and high absorption, limiting its application in areas where a high refractive index is required, such as anti-reflection coating, filters, and waveguides. Thus, exploring new material platforms in the UV region will have far reaching advantages for establishing reconfigurable optical devices for the next generation photonic systems. Currently, we are working on novel PCM based platforms to explore plasmonic effects at UV wavelengths. Our results have shown that large spectral tunability in UV frequencies (250–350 nm) is possible by using Sb_2Te_3 based metasurfaces. One of the fundamental challenges that need to be addressed in UV plasmonics is the generation and detection of UV light sources. The prevailing light source in the UV is characterized by limited operational wavelengths, poor tunability, low output power and higher cost. Whereas UV detectors are low in quantum efficiency and limited in bandwidth of operation. Another critical challenge in UV plasmonics would be the fabrication difficulties associated with extremely small feature size (<100 nm). Moreover, realizing a negative index of refraction in the UV and deep-UV spectral band has technological interest for lithography and imaging applications.

The plasmonics effect in UV and visible regions are highly influenced by the precision in fabrication of these nanoscale subwavelength structures. For the UV region, the feature size is much less than 100 nm and pose great challenges in the tolerance of fabrication errors. Prevailing fabrication methods such as electron beam lithography and focused ion beam lithography can reach a limit of ~5–10 nm in resolution but offering a limited throughput and lower accuracy. Extreme ultraviolet (EUV) lithography is widely used in the current semiconductor fabrication field, and it provides a higher throughput with a better accuracy. For instance, EUV lithography at 13.5nm wavelength will provide a sub 10 nm resolution required for such PCM based UV metasurfaces. New PCM materials are to be explored in the UV region for a low-loss optical response. Such new PCM materials in a nanostructure dimension combined with conventional UV material will enable novel quasi materials with modified optical response of phonons and polaritons, thus developing a new platform for UV plasmonics.

We outlined recent research progress in PCM based reconfigurable nanophotonics together with our works on tunable plasmonics with PCMs. Tunable plasmonics using novel PCM based nanostructures are highly promising due to its diverse functionality arising from capability to change its material and electronic property over a wide spectral range. More specifically, the PCM fabricated nanophotonic structures will pave the way for advancing the functionalities in integrated photonic devices in terms of high reconfigurability, high miniaturization, stability with low power consumption and CMOS compatible fabrication. The UV-VIS spectral region is an area of significant interest for future investigations due to the limited availability of low-loss PCM that possess the necessary properties for advanced reconfigurable nanophotonic devices. Exploring novel reconfigurable devices based on UV-VIS metasurfaces offer a promising alternative to traditional optics based on refraction and reflection, opening a wide range of possibilities for diverse functionality.

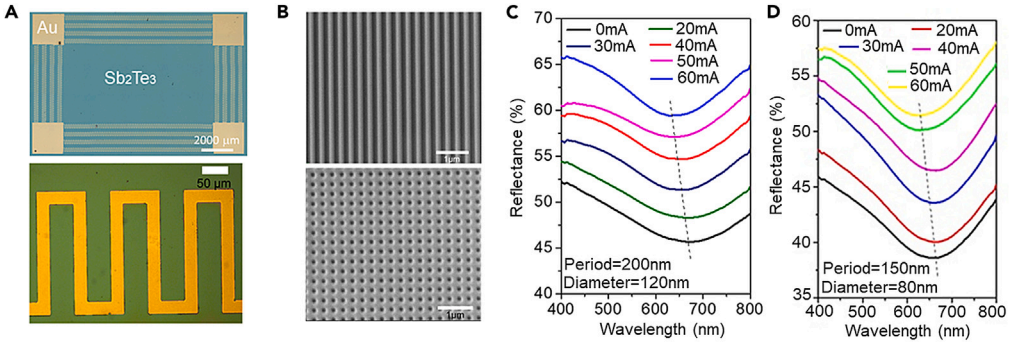

Figure 6. Sb_2Te_3 based metasurfaces and optical properties

(A) Optical microscope image of fabricated microheater integrated Sb_2Te_3/Si PCM device.

(B) Scanning electron microscope image of fabricated Sb_2Te_3 based metasurfaces.

(C and D) Measured reflectance spectra of 2D grating holes with applied current (c) hole diameter = 120 nm and period = 200 nm and (d) hole diameter = 80 nm and period = 150 nm. Adapted from.[85,90,91]

Terahertz reconfigurable photonics with PCM by S.Z., T.C., Z.T.

Due to exceptional properties such as distinct spectral fingerprints, increased available bandwidth, nonionizing nature, and greater penetration depth, THz radiation offers significant potential for applications in biomedical examinations, sensing, communications, and security inspections.[99–102] The advancement of THz devices capable of manipulating THz wavefronts is crucial for facilitating these applications. In recent years, reconfigurable photonic devices utilizing PCMs for THz radiation have gained increasing attention, particularly non-volatile reconfigurable metasurface devices based on $Ge_2Sb_2Te_5$ (GST) which is among the most widely used PCMs. There has been some recent research investigating the potential of utilizing PCMs in THz reconfigurable photonics. Pitchappa et al. were among the first to explore the use of chalcogenide PCMs for active THz photonics.[22] They utilized resonant metamaterial devices integrated with GST to achieve multidimensional control of THz waves. Through varying the annealing time and temperature, they were able to achieve a continuous modulation of THz conductivity by controlling the percentage of crystalline sites. Additionally, the integration of GST with an asymmetric split ring resonator (ASRR) enabled the realization of both two-level (ON-OFF) and multilevel switching of Fano resonance. Subsequently, a 2 × 2 multicolor spatial light modulators for THz spectral band was demonstrated by electrical switching of GST. Each Fano resonance was independently transformed to multiple states. In addition, they exploited the semiconducting nature of GST in the different crystallographic phases to achieve variable ultrafast volatile switching under optical excitation. They further demonstrated a GST integrated Fano resonant meta-device fabricated on a flexible substrate.[103] Based on the power of optical stimulus, either non-volatile switching or volatile switching of Fano resonance was realized. When the optical power was higher than the threshold power, the multilevel non-volatile states were achieved by controlling the optical stimulus power and time. When the optical power was less than the threshold power, the volatile switching was achieved through photodoping of the semiconducting GST film. The research demonstrated the non-volatile phase transition characteristics of GST at the THz regime through thermal, electrical, and optically controlled ultrafast volatile modulation. These findings enabled the exploration of non-volatile reconfigurable THz devices. The crystallization process of GST was achieved using thermal, electric, and optical stimuli. However, the re-amorphization process, which is essential for reversible switching, has yet to be investigated. Figure 7 shows a pictorial representation of the roadmap for THz reconfigurable photonics with PCM.

Liu et al. explored the reversible phase-transition characteristic of GST using thermal annealing and laser pulses.[59–62] Through this research, they were able to incorporate GST into the functional resonator and realize a dynamically reconfigurable electromagnetically induced transparency (EIT) metasurface at the THz regime. Through the control of annealing temperature and modulation of the crystallization ratio of amorphous GST, Liu et al. were able to achieve multilevel modulation of conductivity and group delay. They also demonstrated the ability to perform ten cycles of ON-to-OFF active control of the EIT using nanosecond laser pulses. Following the same approach, Cao et al. presented a non-volatile reconfigurable meta-device for manipulating the extraordinary optical transmission (EOT) effect in the THz region.[104,105] The multilevel modulation of EOT was realized by continuously changing the annealing temperature. They further accomplished reversible switching (ON/OFF) of the EOT through optical pumping. Using more diverse modulation methods, Chen et al. demonstrated reconfigurable and non-volatile THz hybrid plasmonic dimer structure by integrating GST.[53–56] The THz response of GST was characterized by the thermally stimulated crystallization and optically stimulated re-amorphization process. Integrating tunable characteristics and multiple functions into a single metasurface attracted extensive attention. Chen et al. proposed a reconfigurable bifunctional metasurface, which can function as a switch between broadband polarization and absorption.[53–56] Incorporating GST with phase-discontinuities metasurfaces to achieve the phase modulation of THz wavefront is essential for reconfigurable THz functional devices. Zhang et al. combined GST with phase-discontinuities metasurfaces to realize multiple non-volatile reconfigurable THz modulators, including anomalous deflectors, metalenses, and focusing optical vortex generators.[106,107] Repeated switching and multilevel modulation of devices was realized with the help

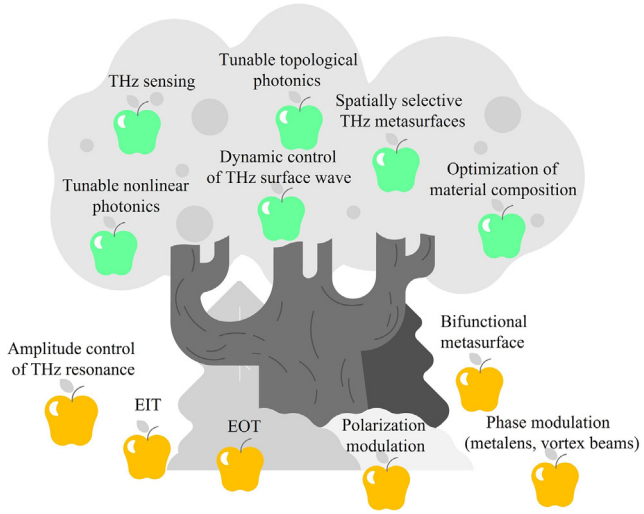

Figure 7. Roadmap for THz reconfigurable photonics with PCM

The metasurface tree shows developments and future of THz reconfigurable metasurface research. The ripe fruits: the research have been reported and realized experimentally. The unripe fruits: the futuristic research that are on the roadmap.

of thermal annealing and optical stimulus. Subsequently, through further optimization of metasurfaces, dynamically switchable THz meta-devices were proposed.[106,107] Temperature tunable EIT in THz frequencies was demonstrated by fabricating metasurface on ferroelectric platform.[108] Through thermal annealing and laser pulses, reversible and repeated switching of multiple devices including the dynamic beam splitter, bifocal meta-lens, dual mode focusing optical vortex generators, and switchable metalenses/focusing optical vortex generators have been realized. However, a critical challenge in this spectral region is the limitation in switching speed when dealing with larger areas of THz PCM devices. Switching methods such as laser and electrical pulse-based annealing are often restricted to small areas, which hinders scalability and affects the overall surface area of the device.

The large wavelength of the THz wave presents challenges for phase transition methods, as the phase transition area of GST can be on the order of centimeters. However, the above research has successfully characterized the THz spectral properties of GST and achieved multilevel crystallization and amorphization processes through thermal annealing and optical stimulus, respectively. The feasibility of optically controlled ultrafast amorphization of GST with a diameter of 1 cm has been demonstrated using a nanosecond laser, and the crystallization process has been shown with an optical stimulus for 10 min. It should be noted that the ultrafast switching from amorphous to crystalline state has not yet been realized in the THz region. The reasons have been illustrated.[53–56,109] Applying more than two optical pulses with a duration of 10 ns can induce the transition from amorphous to FCC (face-centered cubic) phase. However, the FCC to HCP (hexagonal close packed) phase transition process cannot be realized using optical pulses of such short duration. Additionally, inducing switching of GST for large-area devices through electrical pulses is extremely challenging due to the electrothermal effect. However, switching from amorphous to crystalline state is feasible for GST placed in the gap using electrical pulses on the order of seconds. Therefore, achieving ultrafast large-area GST switching under the current phase transition conditions is extremely difficult.

The development of spatially selective, energy-efficient, and ultrafast-responsive THz meta-devices can be achieved by optimizing structure design and material composition in the future. A recent proposal involves integrating GeTe into metasurfaces, allowing for optical control of THz waves.[58] However, the use of contact masks to achieve specific coding functionality and reflective working mode limits their potential applications. Despite the many appealing features of GST, including non-volatility, reconfigurability, high endurance, and high operation speed, its applications in the THz band are still in the early stages. In the future, the development of integrated and optically/electrically addressable THz reconfigurable devices and novel PCM compositions with large contrast, ultrafast response, and moderate energy consumption will be a challenge. Another important goal is the development of various THz reconfigurable photonics devices. The control of THz surface waves is crucial for the realization of THz on-chip systems. Recently, Chen et al. proposed the dynamic surface wave switching at THz regime using a mechanically reconfigurable metasurface.[53–56] Yet, non-volatile reconfigurable generation and shaping of THz surface waves have not been reported. Metasurfaces integrated with GST show great promise as potential candidates for achieving tunable THz topological and nonlinear photonics, which will continue to play crucial roles in advancing the development of next generation cutting-edge THz technology.

Phase change materials for integrated photonics by C-C.P., B.M., T.G., and J.H.

A familiar face in the electronic memory industry, PCM is only a new player in the integrated photonics arena. The recent surge of interest in PCMs for photonic applications is motivated by their unique ability of providing giant, non-volatile optical contrast.[110,111] Conventional electro-optic or thermo-optic modulation mechanisms rely upon miniscule, volatile index changes of the order of 10^{-2} or less. As a result, on-chip

light routing traditionally demands long switching devices that constantly consume electrical power. In contrast, the large index change afforded by structural transition in PCMs enables ultra-compact optical phase shifters. Moreover, PCM devices allow quasi-passive "set-and-forget" operation – only drawing power during switching operation. These singular characteristics underpin demonstrations of PCM enabled on-chip routing,[112,113] optical memory,[19] analog computing,[114] transient photonics,[73–75] among others. The intriguing prospects of PCM integration with PICs prompts the question that we seek to address in this perspective: what advances are still needed before these laboratory prototypes can be transitioned to industry-ready technologies?

Tailoring PCMs for photonics

Classical Ge-Sb-Te (GST) alloys are characterized by strong optical absorption due to their small bandgap and large free carrier absorption, particularly in the crystalline state. The optical loss limits the attainable performance of individual devices, and more importantly, cripple scalable integration in functional photonic systems, since the excess losses quickly multiply in a large-scale PIC involving many switching elements. This shortcoming has spurred the development of a cohort of new low-loss PCMs, exemplified by $Ge_2Sb_2Se_4Te$ (GSST),[9–11,27] $Ge_2Sb_2Se_5$ (Meng et al.), Sb_2S_3,[81] and Sb_2Se_3.[2] For applications in the telecom wavelength range, GSST is suited for intensity modulation due to the low optical attenuation in its amorphous state, whereas the sulfides and selenides are ideal for phase-only modulation benefitting from their bistate transparency.[115]

Building on these pioneering efforts, continuing exploration of new PCM compositions specifically tailored for photonic applications is an area where ample opportunities for promising material innovations are present. Since photonics stipulates requirements on PCMs very different from those for memories applications,[73–75,115] re-examination of previously studied (and even discarded) PCM alloys, possibly leveraging data mining and high-throughput computational techniques, likely will also yield useful discoveries.

On the device application front, several key questions are yet to be addressed to facilitate the adoption of these new PCMs in mainstream photonic platforms. Film deposition processes offering large-area (wafer-scale) uniformity and batch-to-batch reproducibility ought to be validated. Device-to-device and cycle-to-cycle variations of switching parameters should be mitigated. Cycling endurance of the materials must be significantly improved. Moreover, integration processes of these materials with standard silicon photonics platforms needs to be developed and qualified.

On-chip electrical switching: Consistency and endurance

PCMs typically use Joule heating to trigger phase transition. Compared to ultrafast laser switching, integrated resistive micro-heaters offer a more versatile and reliable route toward chip-scale integration of PCM devices. Doped silicon heaters represent a seamless interface for PCM integration with silicon photonic devices (Ríos et al., .[9–11,116]; For SiN platforms, metal, indium tin oxide (ITO) or graphene[112,113,117,118] heaters are potential alternatives.

Consistency of the electrothermal switching process is an open topic calling for more systematic investigations. Specifically, fluctuations of switching parameters (voltage amplitude or electrical pulse duration) from device to device and cycle-to-cycle variations of phase-change behavior must be minimized. The former likely results from variations of PCM material quality or contact and other parasitic resistances of micro-heaters. The latter, which is detrimental to multilevel or analogue operation of PCM devices, could be correlated with stochastic nucleation in PCMs.[20,21] Thorough understanding and mitigation of these mechanisms will be essential for practical deployment of PCM photonics.

High endurance electrically switched PCM photonics is another area where much improvement is necessary. Even though cycling lifetime of the order of 10^6 to 10^8 has been routinely realized in electronic PCM memories and more recently in RF switches,[119] the endurances of PCM photonic devices often remain in the level of a few thousands or even less (Ríos et al. ,[9–11,112,113]; far from the intrinsic lifetime of these materials. While such endurance figures can already fulfill the demand of selected applications such as photonic trimming, transient photonics,[73–75] and reconfigurable optical neural networks with offline training,[115] they fall short of more general photonic switching specifications: for instance, a device that switches only once every minute over a two-year period already entails an endurance of 10^6. An endurance record for PCM photonic devices exceeding half a million cycles has recently been reported (Meng et al.). This important milestone demonstrates the promise of achieving high-endurance PCM photonics through judicious engineering of the heater geometry and material as well as capping layer composition and thickness.[120] Moving forward, systematic studies on various failure modes of PCM integrated photonics and pertinent mitigation strategies will be essential to further performance improvement.

Scalable PIC integration and manufacturing

The maturing ecosystem of photonic foundry manufacturing has qualified fabless photonics as a cost-effective model for introducing new materials and designs into the mainstream PIC industry. Integration of PCMs into the standard integrated photonics fabrication and packaging processes is therefore the rational choice if they are to make significant impacts on practical applications. To their credit, chalcogenides are no stranger to semiconductor manufacturing. For example, Intel's XPoint memory uses a GST-based PCM as the storage element and an As-doped Ge-Si-Se alloy as the selector. In addition, the PCMs can be readily deposited using physical vapor deposition methods at low substrate temperatures, a process compatible with backend-of-the-line integration. A strawman PCM integration process therefore involves foundry tape-out of active PIC chips with embedded doped silicon-on-insulator heaters, opening windows in the top oxide cladding to expose the waveguide heaters at selected regions deposition and patterning of PCM in the oxide trenches, deposition of capping layers and cladding to encapsulate the PCM elements, and finally an additional lithographic patterning step on the cladding to allow access to the metal contacts. In the initial validation phase, steps including and after PCM deposition can

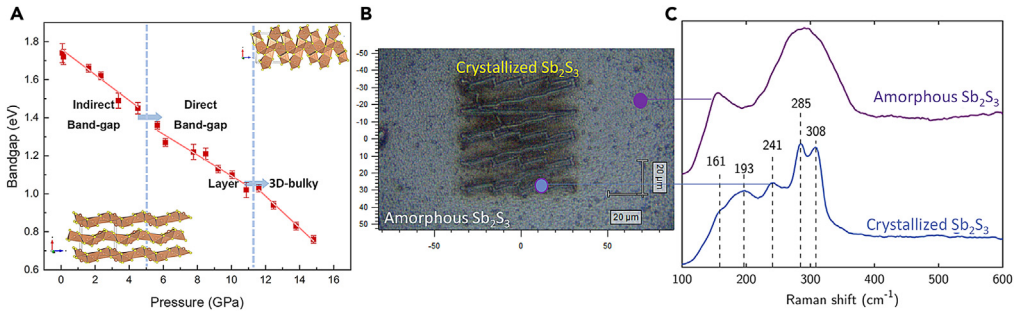

Figure 8. Optical properties of Sb_2S_3

(A) Variation of the optical bandgap of Sb_2S_3 as a function of layered-3D polymorph crystalline-to-crystalline transition occurring by stress/pressure variation. (B and C) 532 nm laser writing of the amorphous-to-crystalline transition, as confirmed by the Raman spectra in (c).

be performed in dedicated facilities. Once the process is vetted and the added values introduced by PCMs are established, the entire process can become part of the standard process design kit (PDK) portfolio offered by one or more leading photonic foundries. Only then can PCM truly claim its spot in mainstream integrated photonics and fulfill its potential in enabling next-generation programmable photonics.

PCM antimonide sulfide (Sb_2S_3) devices by M.L.

In the last few years there has been an incredible increase of interest in antimony trisulfide or antimonite, Sb_2S_3, which is a PCM with good Earth abundance, non-toxic composition, and affordable cost. Sb_2S_3 is an archetypal layered material that contains parallel Sb_4S_6 chains formulated in 2 × 1 crumpled sheets, held up by weak van der Waals forces.[121] The beauty of this layered structure is that several polymorphs crystalline-to-crystalline phase transitions are possible in addition to the amorphous-to-crystalline one, leading to a change of the refractive index and, therefore, optical modulation of light. A set of pressure-induced polymorphic and electronic phase transitions may occur in response to external stress stimuli due to the change of pressure. As an example, an electronic topological transition with a redistribution of charge density near the conduction band maximum (CBM) and a change of bandgap from indirect 1.73 eV to direct 1.35 eV at approximately 4 GPa has been recently demonstrated, whereas a layered-to-3D-bulky structure with a bandgap of 0.68 eV occurs at 11 GPa (see Figure 8).[122] In addition, there is the most commonly exploited crystalline-to-amorphous phase transition with an optical bandgap change from 1.73 eV to 2.05 eV for the amorphous phase, and a refractive index contrast $\Delta n \approx 0.6$ with negligible losses, as the extinction coefficient, k, is less than 10^{-5} in both amorphous and crystalline phases at 1550 nm.[2] Interestingly, the phase transition temperature of Sb_2S_3 has a crystallization activation energy of 2.0 eV,[87,89,92] which is even lower than that of $Ge_2Sb_2Te_5$ (GST)(2.3 eV)[123] making the amorphous-to-crystalline phase transition accessible thermally at T = 230°C and also by green laser diode irradiation[121] (see Figure 8) and near-field probe techniques. Starting from a homogeneous amorphous Sb_2S_3 film, a focused green laser can write an arbitrary pattern by inducing a local phase transition, with the pixel size of the pattern determined by the focal point of the laser.

This makes Sb_2S_3 a good PCM candidate for solar cells,[124] as a promising thermoelectric material,[100–102] while low absorption losses in the near infrared as well as in the visible, make Sb_2S_3 interesting for tunable NIR and visible photonics applications beyond data storage, such as holographic displays[81] reprogrammable visible and NIR light routers and beam steerers.

To design active photonic Sb_2S_3 devices, we need to know the refractive index in both its amorphous and crystalline states, and today this is enabled by the fact that we have determined the spectral dependence of the refractive index of Sb_2S_3 not only for the amorphous and crystalline states but also for various crystallized phases, also depending on the Sb_2S_3 deposition methodology.[121] The truly low-loss switchable refractive index opens new directions in programmable integrated photonic circuits, switchable metasurfaces, and nanophotonic devices, as discussed here.

Reconfigurable photonic devices

Despite the fact that further studies on the cycles endurance and optimization of reversibility of the Sb_2S_3 amorphous-to-crystalline transition are needed, integration of Sb_2S_3 in photonic circuits is already being exploited in the design of reconfigurable photodetectors and silicon nitride Mach–Zehnder interferometers (MZIs) operating in the C and O communication bands.[125]

Photodetectors can be designed based on Sb_2S_3-based metal-dielectric-metal (MDM) cavities. Au-Sb_2S_3-Au works as a hot electron photodetector (HEPD) for tunable for absorption and responsivity in the spectral range 720 nm–1250 nm for the crystalline phase and 604 nm–3542 nm for the amorphous phase. The single resonance cavity and thus the sensitivity of the designed HEPD device can be changed to the double resonance cavity via the crystalline-to-amorphous phase transition. Noteworthy, the maximum predicted responsivities for the single and double cavities are 20 and 24 mA W^{-1}, respectively, at 950 nm and 1050 nm wavelengths which are the highest among all previously proposed planar HEPD devices.[126]

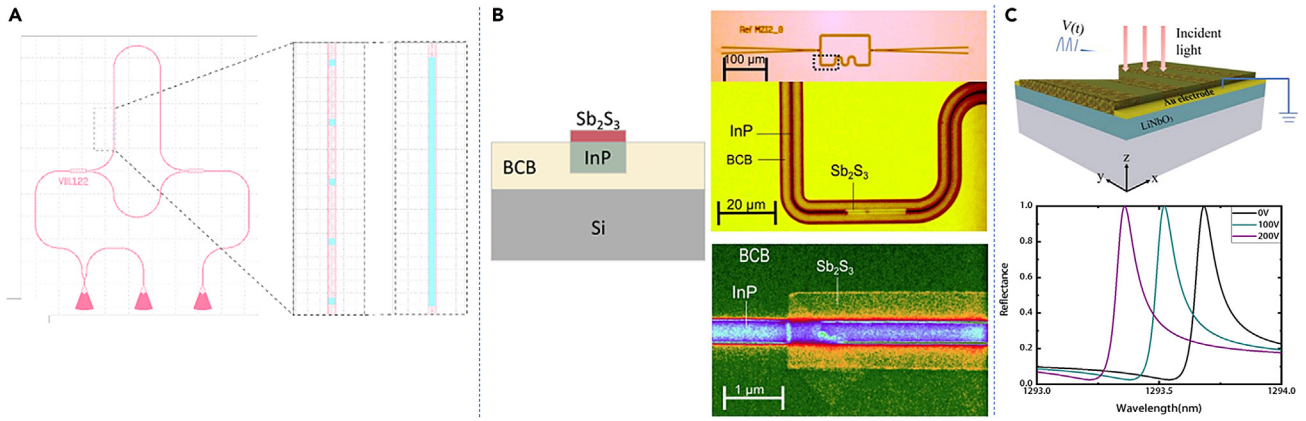

Figure 9. Switchable modulators and metasurfaces

(A) The design of MZI phase modulator equipped with PCM cell atop one of the arms in two configurations: patterned cells and unpatterned cell.

(B) Microscope image of the Sb_2S_3-based MZI device on InP waveguide, with the colorized-SEM image of Sb_2S_3 patterned on the InP waveguide. Adapted from.[130]

(C) Scheme of the resonant Sb_2S_3-LN metasurface with a pair of Au electrodes, with the reflection spectra showing the tunability and the shift of the plasmon resonance with different gate voltage from 0 V to 200 V. Adapted from.[84]

In the context of tunable photonics applications ranging from the visible to the near-infrared region, a reversible and ultrafast (~70 ns) Sb_2S_3 amorphous-to-crystalline phase transitio[127] and a cyclability where Sb_2S_3 can switch up to 7000 times depending on the extent of amorphization[128] have been demonstrated, making Sb_2S_3 suitable for non-volatile phase modulator building blocks in the O and C-bands.

Teo et al.[127] have demonstrated programmable 1 × 2 optical couplers also based on Sb_2S_3 showing the best overall performance, even compared to GST, with the lowest insertion losses of 0.04 dB/μm in both the amorphous and crystalline phases, to design a 2-bit tunable Sb_2S_3 directional coupler with a dynamic range close to 32 dB, where the bit-depth of the coupler appears to be limited by the crystallization stochasticity, pointing out that a better control of the crystallization dynamics of Sb_2S_3 still needs to be achieved. Indeed, our recent studies[121] on the crystallization dynamics revealed that it is not a matter of stochasticity but of the spherulitic and inverted spherulitic crystals that depend on local temperature. Those various crystallized states could enable 2-bit weights in a conceptual Sb_2S_3 programmable photonic integrated circuit (PIC), quantized neural network, which could down-scale deep neural networks in space-limited platforms, such as mobile devices.

Further improvement, of Sb_2S_3 based MZI can be reached by a design we recently proposed[121] consisting in placing the PCM Sb_2S_3 cells in both arms of MZI and antipolar switching of both cells (PCM cell in the one arm in the amorphous state, while PCM cell in another arm – in the crystalline state and vice versa), can be obtained by utilization controllable individual microheaters[129] (see Figure 9).

While most of the studies focus on silicon photonics, where the high thermal conductivity of the waveguide material makes heating the PCM energy inefficient, very recently, a Sb_2S_3-reonfigurable InP waveguide Mach–Zehnder interferometer (MZI) to make an optical switch in the telecoms conventional-band achieving 18 dB on/off switching at 1540 nm has also been demonstrated.[130]

Additionally, switchable metasurfaces combining Sb_2S_3 as a subwavelength refractive index grating on top of lithium niobate (LN) are being proposed, as shown in Figure 9. Such a refractive index grating is comprised of periodical distributions of amorphous and crystalline Sb_2S_3, which can be "written", "erased" or "rewritten" with a customized writing beam (laser or ion). Simulation results show that the resonant Sb_2S_3-LN metasurface has extremely narrow linewidth and high Q factors. The optical spectra can be continuously tuned by not only the duty cycle of the grating, but also the crystallization fraction of the switched Sb_2S_3. Combining with the nonlinear and electro-optical properties of LN, the hybrid metasurface provides an unprecedented possibility of active nanophotonics such as nonlinear propagation and electro-optical control.[84]

Challenges and perspective

Despite the presented devices, challenges associated to the integration of Sb_2S_3 with a commercial production line, the stability over time, and practical stimuli for the phase transition will drive future research, as there is still need for more research to further improve the cyclability and the energy savings to make the PCM Sb_2S_3 competitive with conventional GST.

Cycling endurance. A major challenge for integrating Sb_2S_3 in devices is its stability. An Sb_2S_3 film would segregate antimony (Sb) upon high temperature (T > 300°C) treatment so that the devices usually suffer from a limited number of cycles reproducibility, causing a drift in the response. A common way to solve or reduce this issue is the use of encapsulating protective layers, such as ZnS: SiO_2 to prevent sulfur loss and reduce Sb-segregation. More studies on the role of the capping layer in the dynamics of the phase transition are also needed.

Multi-level optical states. The control of phases and of the crystallization fraction will enable more degrees of freedom in the design of multi-functional devices. All the applications considered so far are binary, i.e., all have two states amorphous/crystalline, whereas controlling the percentage of the phase transition locally would enable neuro-inspired computing. Intermediate switching states by partial amorphization or progressive crystallization under optical excitations by combining multiple optical pulses with various amplitudes, widths, and time intervals, could be implemented to create crystalline pixels along the waveguide length as a desirable feature of reprogrammable couplers. We could also envisage including an embedded heater below the Sb_2S_3 PCM, but a proper thermal design needs to be implemented.

Speed of transition. Better control of the material engineering, including doping and alloying could contribute to lower the transition temperature, or to enable new phases or allow mechanically and electrically activated phase transitions, such as polymorph crystalline-to-crystalline transition by strain modulation or electronic transition by electron redistribution, which have the potential to improve the speed of the phase transition.

Power consumption. Reducing power consumption is another step toward practical applications. This is especially true for the crystalline-to-amorphous reverse transition when high power heat pulses are needed to melt-quench the material from crystalline to amorphous. To reversibly switch Sb_2S_3 it must be heated above its 550°C melting temperature and then quenched into its amorphous phase. This could introduce some damage not only into the material but in the device. Therefore, strategies are needed to improve the energy efficiency of the laser-induced amorphization by inserting appropriate thermal barriers to efficiently confine energy within the PCM layer. As an example, very recently, a layer of two-dimensional (2D) material, either MoS_2 or WS_2, between the silica or silicon and the PCM has been reported to reduce the required laser power by at least 40% during the amorphization process.[131]

Plasmonic coupling. To further extend the reconfigurability of the working frequency from telecom to the UV-visible spectral range (500-300 nm) tunable plasmonic responses of nanostructured Sb_2S_3 and of integrated plasmonic structures are exploited. The plasmon resonance of gratings of Sb_2S_3 can also be considered a design parameter for tuning the Sb_2S_3-based optical devices. Additionally, the crystallization/amorphization of Sb_2S_3 can be used to control the surface plasmon resonance of plasmonic nanostructures, to confine surface phonon polaritons and to create active metamaterials.

Manufacturing. From a device manufacturing point of view, Sb_2S_3 requires optimization of recipes for dry etching and cleaning processes. Furthermore, the possibility to integrate both pump and probe optical pulses on chip would be needed to reduce footprints, switching speed and energy consumption.

Thus, to achieve the goal of phase-change photonics on various platforms, it is important for the understanding of material properties of PCMs to more complex situations occurring in devices, which include interface effects, stoichiometric variation, aging, stress relaxation, extensive cycling, nano size effects, complex pulsing schemes with consideration also of non-isothermal and non-equilibrium conditions.

Programmable silicon photonics based on phase-change materials by Z.F., R.C., A.M.

Silicon photonics has evolved from lab research to commercial products in the past decade as it plays a more crucial role in next-generation large data centers.[132] More recently, it has also found niche applications in optical neural network,[133] quantum information processing,[134] and light detection and ranging.[135] Despite the progress, most silicon PICs still rely on thermo-optic and carrier dispersion effect to tune the circuits, which are weak, volatile, and power hungry. In order to overcome these limitations, PCMs offer a viable solution which promises zero-static power consumption and enormous index contrast ($\Delta n \sim 1$).[112,113] Here, we review the recent progress and challenges in the field of programmable silicon photonics based on PCMs and discuss the technologies necessary to tackle the challenges.

Modulation, either of light phase or amplitude, is a fundamental building block for programmable PICs. For certain applications such as optical modulators, the modulation needs to be fast and is generally realized via carrier dispersion[136] or electro-optic effect.[137–139] On the other hand, tuning of the PICs, such as light routing and trimming, only requires slow speed and is traditionally achieved by micro-electro-mechanical systems (MEMS)[140] and thermo-optic effect. The drawbacks of these methods are their volatile nature – a constant power or bias must be applied to maintain the state. The static power consumption, not contributing to the active tuning of the PICs, becomes dominant. It is hence highly desirable to have a "set-and-forget" type switch to tune the PICs, requiring no static power or bias. Chalcogenide-based PCMs, exemplified by the technologically mature $Ge_2Sb_2Te_5$(GST), are well-studied in the random-access memory (RAM) and optical storage community[141] and hence can provide a feasible route to achieving such "set-and-forget" switch. The modulation is achieved by changing the PCM between its amorphous and crystalline phases (which have vastly different optical properties) via heating by optical or electrical pulses. The first demonstration of a PCM-based silicon photonic switch was realized on a GST-clad micro-ring resonator which was switched by a free-space laser.[142] Later studies[12,19,143] showed that GST is an ideal material for integrated photonic memory and amplitude modulation since it undergoes a gigantic change in optical absorption (>1 dB/μm) upon their material phase transition. However, this also implies that GST is a lossy material, prohibiting its use in phase-only modulation - essential for post-fabrication trimming and arbitrary linear optics. Although device engineering could to some extent circumvent losses,[27,53–56,144] such a fundamental limit of GST prompts the active search for low-loss PCMs,[2,9–11,81] which are not necessarily the best candidates for electronic memory in the early days. Sb_2Se_3 and Sb_2S_3, in particular, exhibit low-loss in both amorphous and crystalline states in the C band and O band, making them ideal candidates for phase-only modulation in silicon photonics.[82,145]

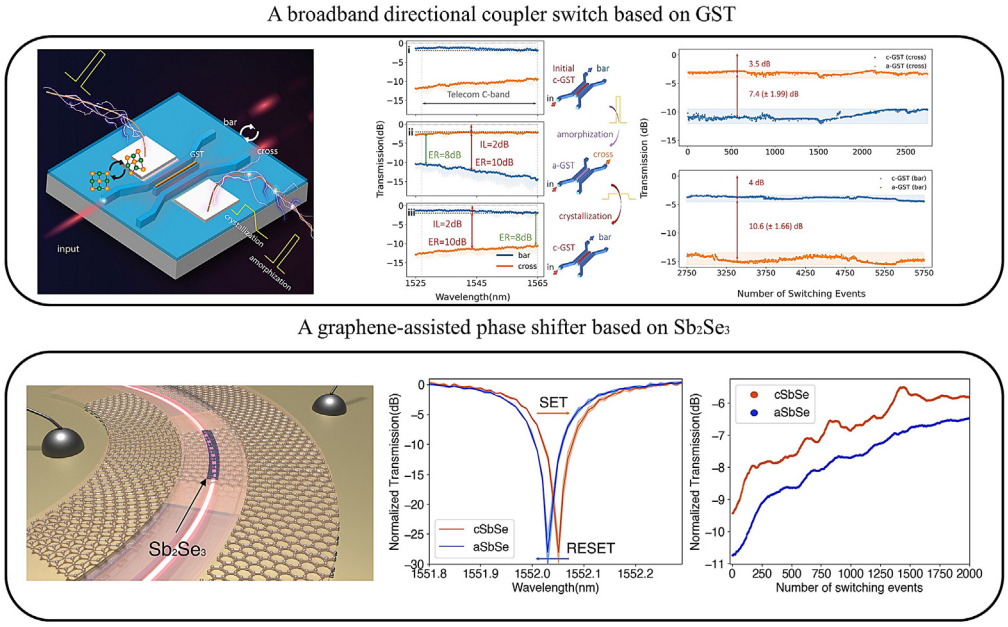

Figure 10. (top) A broadband 2×2 silicon photonic switch based on GST and doped silicon PIN heaters

Adapted from Chen, Rui et al. "Broadband Nonvolatile Electrically Controlled Programmable Units in Silicon Photonics." ACS Photonics 9.6 (2022): 2142–2150. (bottom) A low-loss phase shifter based on Sb_2Se_3 controlled by a graphene heater. Adapted from Fang, Zhuoran et al. "Ultra-low-energy programmable non-volatile silicon photonics based on phase-change materials with graphene heaters." Nature Nanotechnology 17.8 (2022): 842–848.

Although optically switching PCMs offers a fast and convenient way to tune the PCMs without inducing additional losses to the PICs,[12,19,143,145] recently the field has moved toward electrical switching which promises better scalability. Various heater materials for actuating the phase transition in PCMs have been tested, such as ITO,[82,146,147] doped silico,[9–11,53–56,116] metals,[148–150] and graphen.[112,113,117,118] The most promising ones are silicon PIN[53–56,116] and graphene,[112,113] where high switching endurance (>2,800 cycles), broadband operation, phase-only modulation, and ultralow switching energy are recently demonstrated (see Figure 10). Leveraging on these advancements in electrical control, a plethora of active PIC building blocks has been realized, such as phase shifters (Ríos et al. ,[112,113]; micro-ring switch,[82,116] and broadband directional coupler switch.[53–56]

The ultimate goal for PCM-based programmable silicon photonics is to create large-scale generic PICs that can be programmed to be used for any desired functionalities. To create such an optical programmable gate array, akin to the electronic field-programmable gate array (FPGA), several crucial challenges must be addressed.

1) First, switching voltage must be reduced to CMOS level (<1V). Although recent progress in silicon PIN[116] and graphene[112,113] micro-heaters have achieved low voltage switching (<5V), switching large and thick PCMs to attain full π phase shift remains to be challenging with low voltages (Ríos et al.).
2) Secondly, current GST-based silicon photonics still suffers from high insertion loss (IL) (>1dB) and low extinction ratio (ER) (<10dB). Wide bandgap PCMs such as Sb_2S_3 and Sb_2Se_3 can reduce the insertion loss below 1dB but achieving <0.1dB IL and >30 dB ER simultaneously proves to be more difficult.
3) Third, analog or multilevel operation of electrically tunable PCM devices remains elusive. Recent work has demonstrated 14 distinct phase levels using a graphene heater,[112,113] but still far less than what has been achieved using optical switching[151] and suffers from large state variations.
4) Fourth, device endurance still must be improved. While commercial products normally require cyclability of >1 billion cycles,[152] the highest endurance demonstrated in silicon photonic devices is only half a million cycles at high driving voltage (>10V).[148–150]
5) Lastly, PCMs must be made fully compatible with the current silicon photonics foundry process to realize wafer-scale manufacturing. Although companies like Intel and IBM have already had PCMs such as GST in their foundry for RAM devices, introducing new PCMs into silicon photonics foundry will be more challenging due to drastically different chemical and physical processes involved in the fabrication.

A few strategies can be adopted to address the above challenges. To begin with, further reduction of switching voltage below 1V requires the co-optimization of microheaters both electrically and thermally. In the case of silicon PIN heaters, the doping profile, concentration, location (distance between the doping and intrinsic region), and the silicon slab waveguide thickness all need to be carefully designed to achieve low resistance heaters while not inducing significant optical losses. If a graphene heater is used, graphene transfer must be optimized to avoid

wrinkles and ruptures so that the sheet resistance can be reduced. Mechanical transfer of graphene sandwiched by hexagonal boron nitride[153] was shown to be effective at obtaining low sheet resistance. Meanwhile the contact resistance should be minimized to increase the voltage drop across the graphene heater region. To achieve this, one-dimensional edge contact can be used.[154] Low switching energy can also be realized by using thick capping layer which reduces the heat dissipation from the PCMs but will lead to trade-off in switching speed. Secondly, low IL and high ER require the discovery of new wide bandgap PCMs with large refractive index change ($\Delta n > 1$). High ER can also be realized by switching large volumes of PCMs (>50 nm thickness) where PCMs with slow phase change kinetics can have an advantage.[9–11] Mode mismatch between the bare waveguides and the PCM-loaded waveguide can also incur additional scattering losses, where engineering the shape of PCM patch into tapers may help to reduce such loss. Third, deterministic multilevel operation can be realized using segmented heaters where *n* independently controlled heaters are used to express *n+1* levels and each PCM patch is switched in a binary fashion. However, this approach will lead to an increased number of electrical leads and hence complexity in control. Alternatively, analogue tuning can be achieved by using growth dominated PCMs such as Sb_2S_3[127,128] which requires multiple pulses to fully change the states, where the number of levels are determined by the number of input pulses. The drawback is that such a method relies on the stochastic nature of phase transition and deterministic operation may require complex pulse engineering. Further, device endurance can be potentially improved by either thermal engineering or using thicker and denser atomic-layer-deposited (ALD) Al_2O_3 capping. One failure mechanism of PCM is the PCM ablation caused by localized hot spots. The hot spots can be a result of non-uniform doping or uneven surfaces, and the higher temperature at the heater center. Material ablation at the hot spots can easily occur during amorphization which requires heating the entire PCM above the melting point. Engineering the shape of the heater can help to reduce the thermal non-uniformity.[73–75] Another method is to use a heater much wider than the PCM area to ensure the PCM lies in the region where the temperature is uniform. One common failure mechanism originates from the reflowing of the molten PCMs during amorphization. PCMs segregate into small islands due to the reflow and consequently the same pulse conditions can no longer cause switching.[53–56] Thicker (>100nm) and denser ALD Alumina encapsulation can potentially prevent the reflowing. Nano-patterning PCMs into smaller (subwavelength) sizes has also been shown to mitigate reflowing.[143] Finally, foundry compatibility can be motivated and accelerated by a growing interest in PCM-based silicon photonics from more research groups. Since a wafer is usually shared among multiple research groups, a larger demand for PCM-related processes, such as deposition and etching, will make it more attractive for the foundry to open up a dedicated line for PCMs. Moreover, demonstrating a commercially relevant silicon photonics product based on PCMs may also help to draw attention from larger companies such as Intel and IBM which can help to push the PCMs into their silicon photonics fabrication line.

Overall, PCMs can provide an attractive solution for the "set-and-forget" tuning in silicon photonics, while enabling compact device footprint and high energy efficiency. Although tremendous progress has been made to improve the performance of the PCM-based devices, remaining challenges, such as endurance, CMOS-level voltage control, low insertion loss, high extinction ratio, multilevel operation, and foundry compatibility must be resolved before the PCM approach can provide practical solutions to a large-scale programmable gate array. We have identified several potential opportunities to address these challenges.

Chalcogenide photonic integrated circuits for reconfigurable and nonlinear functionality by C.K.L., M.M. and B.J.E.

Pursuing optical materials and devices with exceptional tunability has been one of the key priorities in the field of integrated photonics. Thus far, chalcogenide glasses (ChGs), which are composed of one or more chalcogens (S, Se, Te) and other network formers such as As, Ge, Sb, Ga, Si or P appear to be the perfect candidates for fulfilling such a vision owing to its capability of demonstrating a wide range of optical properties.[155] By tailoring ChGs' material constituents and glass composition, they can be engineered to possess high photosensitivity, wide infrared (IR) transparency window, thermally driven solid (amorphous) – solid (crystalline) phase change characteristics, and large optical nonlinearity. These striking features have prompted a series of research activities ranging from waveguide writing, post-fabrication grating inscription,[156] mid-IR devices — supercontinuum generation and spectroscopy, non-volatile memory devices, non von Neumann (in-memory and neuromorphic) computing, to various types of nonlinear optical effects — Kerr, four-wave mixing, stimulated Raman scattering (SRS), stimulated Brillouin scattering (SBS) to name a few.

The last decade has seen a drastic growth of chalcogenide PICs, particularly in the context of PCMs and SBS. These PICs sought to provide high-performance reconfigurable optical signal processing units, which can eventually replace their electronic counterparts. Chalcogenide PCMs — GST, GSST, Sb_2S_3 and Sb_2Se_3 systems — undergo a phase transition and large refractive index change when heated.[142,145,157] Employing this unique feature in PICs can result in the development of non-volatile photonic switches that can provide a significant step forward in realizing energy-efficient programmable gate arrays, optical computing and memories.[111] Despite the good prospects, PCMs are generally lossy in the near-infrared regime ($\sim 10^1$ dB/cm) and not suitable to be used as the backbone of PICs — "waveguides". In contrast, ChG such as As_2S_3 has already been processed into waveguides with relatively low propagation losses (~0.2 dB/cm) and reasonably high Kerr and SBS nonlinearity ($\sim 7 \times 10^{-10}$ m/W).[158] SBS, a coherent light-sound interaction in nonlinear waveguides, has seen unprecedented success in the area of integrated microwave photonics.[159] However, monolithic ChG waveguide structures offer limited access to mature component libraries compared to CMOS foundries. Also, they can easily suffer from coupling losses and pump back reflection at the fiber-chip interfaces, which limit the device performance and pose challenges for nonlinear signal processing architectures/functionalities.

High losses, excessive power consumption, lack of versatility and active electro-optics (EO) components, and large device size are undeniably the detrimental factors that motivate a rapid shift toward heterogeneous integration schemes. Recent research efforts have been focusing on exploring heterogeneous architectures where ChGs are deposited in CMOS-compatible photonic systems to achieve practical applications. These include the deposition of tiny strips or metasurfaces of chalcogenide PCMs onto popular platforms such as silicon on

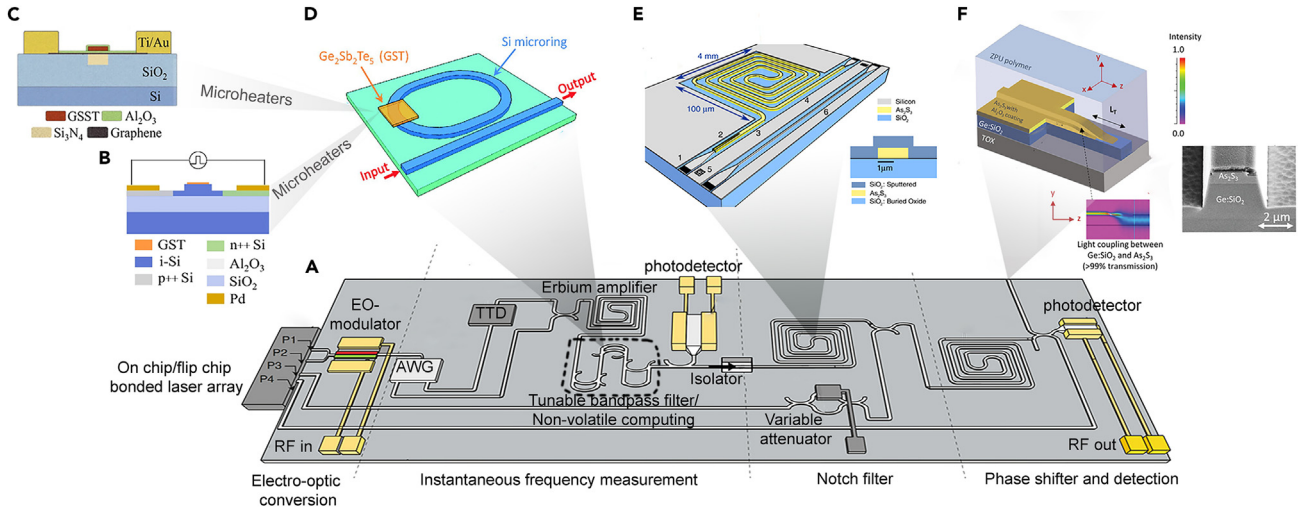

Figure 11. Fully integrated and reconfigurable microwave or optical signal processor

(A) The proposed architecture incorporating tunable bandpass filtering or non-volatile computing, microwave photonics signal processing, linear isolators and some active on-chip components such as lasers, EO-modulator, arrayed waveguide grating (AWG), true time delay (TTD) unit, Erbium doped amplifiers, and photodetectors, Adapted from.[163]

(B) Silicon PIN diode heaters, Adapted from.[116]

(C) Graphene microheater, Adapted from,[117,118] licensed under a Creative Commons Attribution (CC BY) license.

(D) Chalcogenide PCM coated waveguide, Adapted from.[142]

(E) Nonlinear SBS waveguide, Adapted from.[161]

(F) Vertical taper technology for off-chip coupling, Adapted from.[162] Figures and insets adapted from the ref. [116–118,142,161–163].

insulator (SOI),[142] silicon nitride (SiN),[125] indium phosphide (InP),[130] or lithium niobate (LN).[84] The challenges of these proposed PCM hybrid systems lie in the micro-heating strategies[116–118,160] to maximize the switching efficiency and speed, as well as the cycle's endurance. To achieve that, further optimization on minimizing the thermal resistance while keeping the waveguide losses low after the addition of heating pads is necessary. From the perspective of nonlinear PICs, chalcogenide waveguides have been seamlessly interfaced with the standard SOI systems via adiabatic mode transition.[161] It is also worthwhile to highlight that the recent advanced taper technology has enabled smooth chalcogenide vertical tapers to be overlaid on a lower index contrast platform, thus delivering negligible mode overlap losses and back-reflection at the material transition and the fiber-chip interface.[162]

Ultimately, one can expect that a fully reconfigurable and nonlinear chalcogenide PIC will comprise a plethora of heating pads and passive couplers as shown in Figure 11. Meanwhile, further development of active optoelectronic components — lasers, amplifiers, and photodetectors — in such a system also cannot be neglected. While there has been excellent progress in establishing these components driven by the market of telecom networks,[132] LIDAR and sensing,[164] the long existing question as to whether there is a single platform that can provide most components required in chalcogenide PICs yet remains unsolved.

We provide a table showing some key photonic aspects of a few emerging base platforms for chalcogenide PICs (see Table 1). Silicon is certainly a dominant platform for integrated electronics, and the existing research and manufacturing infrastructure is vast, which can be utilized in the field of SOI-integrated optics.[132] The large index contrast and fiber-pigtailing technologies offer extra advantages for compact and low-cost devices. Active effects are also possible through carrier-injection effects and thermo-optic mechanisms, and photodetectors can be integrated through germanium epitaxy.[132] There has also been considerable effort and positive results in the use of flip-chip techniques to integrate laser technology onto SOIs.[132] This makes it naturally a strong contender in many applications in which mass production is an important factor. By leveraging these advantages, we have demonstrated an integrated microwave photonic notch filter by interfacing As_2S_3 nonlinear waveguides with the foundry-produced active silicon photonic chip.[166] The optimization of the backend-of-line process in this work represents a major milestone toward a fully integrated chalcogenide device.

InP photonics, the rival of silicon is also believed to provide compelling advantages when it comes to the level of monolithic integration.[167] The active and passive functions in such a III- V material have proven to be challenging as it requires multiple epitaxy steps to achieve different bandgaps/lattice constants. Despite those challenges, Infinera Corporation has delivered a versatile and densely integrated InP system for high-value devices (e.g., >100 GB/s DWDM transceiver chips). It is also interesting to note that recent research has promoted the use of InP in SOI systems.[168] Whether it is physically or commercially viable to develop the processes, materials, technology and required level of device performance for incorporating chalcogenide PCMs and nonlinear PICs in the InP/SOI platform is however another question completely.

Lower index contrast glasses — doped silica[162] and SiN — offer some relief from issues such as poor coupling efficiency to off-chip devices, linear and nonlinear absorption, though at the cost of less functionality and bigger device size. However, the erbium ion implanting

Table 1. Popular material platforms for heterogeneous integrated chalcogenide photonics (adapted and modified from[2,165])

Aspect	Doped silica ($Ge:SiO_2$)	Silicon nitride (SiN)	Silicon-on-insulator (SOI)[a]	Indium Phosphide (InP)	Lithium niobate ($LN/LiNbO_3$)
Refractive index @ 1550 nm	1.5	2.1	3.5	3.1	2.21 (o), 2.14 (e)[b]
Bending radius (μm)	10000 — 500	50 — 150	5 — 100	100	80
Loss @ 1550 nm (dB/cm)	0.003 — 0.2	0.01 — 0.2	0.1 — 3	1.5 — 3	0.027
Fibre-to-chip coupling loss (dB)	Negligible	0.5	2	3	0.5
Nonlinear index (m^2W^{-1})	2.7×10^{-20}	2.6×10^{-19}	4.5×10^{-18}	1.5×10^{-17}	1.8×10^{-19}
Two-photon absorption ($cm\ GW^{-1}$)	Negligible	Negligible	0.25	60	N/A
Modulation bandwidth and technology	N/A	30 GHz with graphene 33 GHz with PZT	30 GHz with free-carrier plasma dispersion	55 GHz with QCSE-EAM	175 GHz with Electro-optic modulation
Detector	Flip chip or 2-D Materials	Flip chip or 2-D Materials	Ge (50 GHz)	40 GHz	N/A
Optical amplification	N/A	30 dB (Erbium ion implant)	N/A	>20 dB (laser output)	N/A

[a]including nanowires and shallow etched ribs.
[b]o/e denotes the ordinary and extraordinary axis of the $LiNbO_3$ crystal; EAM, electro absorption modulator; PZT, lead zirconate titanate; N/A, not applicable.

technology in SiN demonstrated lately has again boomed as a powerful tool in PICs, allowing a record-breaking 30 dB on-chip signal amplification which could potentially lead to lossless and large-scale programmable circuits.[59–62] Finally, thin-film lithium niobate (LN) has also received enormous attention and interest owing to its excellent electro-optic, all-optical nonlinearities and acousto-optic effect.[169] Not only do these features enable frequency comb generation and various modulation schemes, but also open opportunities to high-performance non-reciprocal devices — a highly demanding component that protects the on-chip lasers from unwanted reflection.

We have discussed the status of chalcogenide PICs and the promising platforms for ChGs to integrate with. We recognize that there is no single base platform that can accommodate all functionalities required for realizing the desired chalcogenide PICs (microwave sources and signal processing, non-volatile memory, optical computing etc.) and thus research efforts should be put into exploring the heterogeneous integration of diverse material systems.

Ultrafast and non-volatile all-optical switch enabled by all-dielectric PCM by H.T., Y.W., Q.H., Y.L., Z.L. and X.M.

The development of computer and internet technology is accompanied by the continuous growth of data processing and transmission rates. However, current optoelectronic hybrid system is restricted by the existence of "electronic bottlenecks", which limits the further improvement of the data exchange rate,[170,171] so the concept of all-optical computing and all-optical communication has emerged. All-optical switches have been extensively studied as one of the fundamental components. Chalcogenide materials have attracted much attention in the field of all-optical research due to their non-volatility and reversible phase transitions induced by laser pulses or electrical pulses. As the most typical chalcogenide material, $Ge_2Sb_2Te_5$ (GST) can be reversibly switched between two stable states, amorphous and crystalline. While for most solid-state materials, their amorphous and crystalline phases have very similar optical properties, PCMs exhibit significant contrast in refractive index (n) and extinction coefficient (k).[172–175]

Phase change all-optical device based on Fano resonance

Photonic devices based on PCMs can be divided into two types: on-chip and free-space systems, and phase-change photonic devices in free-space systems are mainly based on the plasmon resonance of metal materials to control light.[176–180] However, since it is based on metallic metamaterials, high loss of metal increases the device loss and high conductance of metal weakens the thermal accumulating for the transition process, which may have negative effect on the device switching speed.[181] Dielectric materials have lower losses, which can also decrease the thermal loss due to its lower thermal conductance. All-dielectric phase-change photonic devices use the Fano resonance effect to realize the modulation of a specific frequency spectrum. Such as a GST region onto the waveguide of the micro-ring resonator and modulated the state of GST by applying laser illumination from the free spac.[142] This modulation changed the effective refractive index of the waveguide, leading to the control of the resonance wavelength position and achieving the switching function. We have provided a Table 2 to show the latest advancements in the field of phase-change optical switches.

Therefore, we investigate an ultrafast and non-volatile all-optical switch enabled by all-dielectric PCM and photonic crystals (PhCs). A periodic structure is etched on the top layer of SOI silicon, PCM and dielectric material film are stacked on the Si layer, as shown in Figure 12. Similar to hybrid plasmonic metamaterials,[182,183] the dimensions and the refractive index (or dielectric constant) of PhCs surface can influence

Table 2. Statistical summary of the latest advancements in phase-change optical switches

Aspect	PCM/si microring	PCM/Mach-Zehnder	PCM/silicon PIN diode	PCM/Au metasurface	PCM/All-dielectric photonic crystal
Insertion loss	2.5 dB	25dB	N/A	N/A	2.8 dB
Response times	5 us	<400ns	N/A	50 ns	4.5 ps
switching cycles	100 times	>2000	1000 times	50 transition cycles	10^{12} times between two states
On/off ratio	12.36 dB at 1550.384nm	26.7 dB at 1554.1nm	14.7dB	4dB	5.4 dB at 1550 nm; 7.4 dB at 1580 nm

the Fano resonance frequency.[52] Thus, by tuning the structure dimension and surface refractive index, the spectrum of the device may red- or blue-shift so that the selection of the switching wavelength and the switching function can be finely realized. The proposed structure uses ultra-thin PCM as dynamic components, which means that the phase change process can be achieved by using a laser with a lower energy level. The periodic design of nanoscale circular hole enables switching functions in a very small area, which has the advantages of high integration and multiplexing in free space.

Current and future challenges

From an industrialization point of view, it adapts to modern CMOS integrated technique, which makes massive manufacture possible. By integrating with optical waveguide, the device can be more practical for all-optical communication. The signal transmission of "node to node mode" in optical communication can be safer and more efficient. Cycling number of GST can be trillions of times,[109,184,185] thus the theoretical lifetime is much longer than some other similar devices.

However, the light transmittance in the on-state is still limited by the intrinsic extinction coefficient of PCM, which hinders the switching contrast ratio (~20dB) close to practical devices. Exploring PCM with smaller losses (such as GSST) and improving structural design to improve contrast are possible solutions. Another challenge for ultrafast and non-volatile all-optical switching enabled by all-dielectric PCM is the need for a mature, matched laser control system, which is essential for realizing the integrated control of multiple optical circuits, ensuring the stable phase transition cycles of the PCM, and improving the durability of the device.

The high-speed and low-energy characteristics of phase-change optical switches make them crucial components for future photonics-based logical operations. With the continuous advancement of phase-change optical switch technology, we can anticipate their widespread applications in areas such as photon logic gates, optical storage and computing, optical communication networks, and quantum computing and communication. Moreover, the progress in integrated optoelectronic chip technology will facilitate the integration of optical switches with other photonic devices, enabling highly integrated optoelectronic systems. This will provide faster and more efficient solutions for information processing and communication in the future. However, further research and technological breakthroughs are necessary to enhance the reliability, stability, and integration level of phase-change optical switches. It is believed that in the near future, phase-change optical

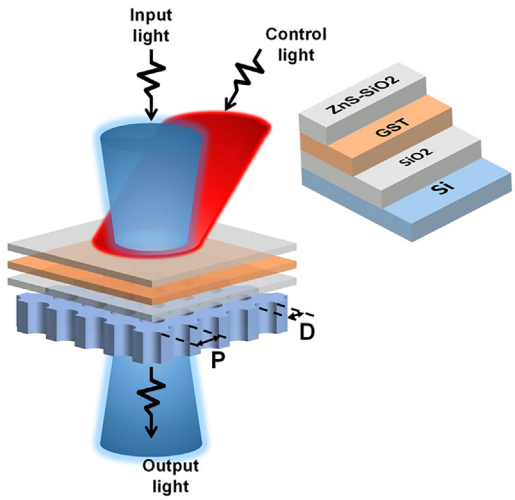

Figure 12. Operation principle of the proposed phase change all-optical switch

The phase change materials thin film is sandwiched by ZnS/SiO_2 and SiO_2. Laser pulses control the phase transition between amorphous and crystalline states, which show dramatic refractive index difference. The resonance wavelength can be finely tuned by changing dimeter D and period P.

switches will play a significant role in logical operations, bringing about revolutionary changes in photonics-based computing and communication.

Reconfigurable phase change photonic metasurfaces by A.M., Y.C., A.S.A., V.B. and B.G.

Metamaterials are composite materials artificially engineered with unique electromagnetic properties not found in naturally occurring materials. Initially conceived as a paradigm to design novel electromagnetic properties, unachievable through traditional chemical formulations, the metamaterial concept has seen rapid growth in many scientific fields and applications ranging from nonlinear nanophotonics to biomedical assays. The unprecedented electromagnetic phenomena exhibited in metamaterials arise from sub-wavelength periodic and/or non-periodic metamolecule resonators embedded within a host medium of a particular chemical composition. Deliberate micro/nano-structuring of the geometrical resonator design and specific formulation of material stoichiometries aid to elicit remarkable electromagnetic behavior because of the engineered effective permittivity and permeability, and by extension the refractive index. Initial THz frequency optical metamaterials were demonstrated with the use of plasmonic metals, such as gold, silver, and aluminum, to enable the engineering of optical wavefronts through the extreme confinement and localization of light, induced by the resonant excitation of conduction electrons – plasmons. All – dielectric metamaterials based on Mie resonances – creation of electric and magnetic dipoles in dielectrics – provided an alternative mechanism for achieving high confinement of light at subwavelength scales; thus, avoiding the ohmic losses associated with the plasmonic platform. Well-documented metamaterial behaviors include negative refractive index with implications for invisibility cloaking applications, perfect absorption for high-efficiency imaging and detection systems, and ultra-thin meta-lenses to realize compact and aberration free optical systems.[186] In the past decade, significant research interests have shifted focus to transforming the passive and static nature of classical metamaterials into tunable and adaptive metadevices. These metadevices have incorporated reconfigurable materials within the subwavelength metamolecule framework to alter their electromagnetic properties in the presence of an external stimuli.

The transformation of passive metamaterials into active metadevices serve as foundational building blocks to tackle current and emerging challenges in applications such as information transfer, signal processing, sensing, imaging, and display technologies. Active tunability of metamaterial properties can be differentiated into two categories: altering the physical geometry of the subwavelength resonators or modulating the permittivity/permeability of the surrounding media through the incorporation of a functional material. Geometrical alterations of the resonant structure can be further subdivided into two approaches: by changing the near-field interaction between adjacent periodic resonators or by changing the shape and dimensions of individual resonators itself. These approaches are one of the initially demonstrated solutions for achieving reconfigurability in plasmonic and metamaterial-based devices. The ubiquitous split ring metamolecule has been fabricated on stretchable membranes, thermal and magnetically driven cantilevers, electro-static platforms, and piezoelectric actuators, to illustrate resonant frequency tunability through physical displacement.[187] Modulation of the inherent electromagnetic properties of the surrounding media has also been proven as an effective method of changing resonant conditions in both plasmonic hybrid and all-dielectric metamaterials. Such examples include the thermo-optic effect (temperature dependence of refractive index), free carrier concentration modulation (refractive index change due to the accumulation or depletion of charge carriers), non-linear electro-optic effects such as Pockels and Kerr effect, and phase transition materials with markedly different refractive indices between two distinct material states (vanadium dioxide, gallium, and liquid crystals).[138,139] One significant drawback underpinning these approaches lie in the inherent volatility associated with the switching mechanism, requiring constant energy input for operation.

This has compelled researchers to explore a non-volatile, bistable, and reconfigurable material platform to meet the needs of next-generation information processing and telecommunication advancements. Chalcogenide phase change materials (ChG - PCM) – compounds containing group 16 or 'chalcogen' elements of the periodic table such as sulfur, selenium, and tellurium, are the most promising material platform to meet these requirements. Since its early implementation as an optical data storage medium in CDs/DVDs, phase change chalcogenides have gained popularity among emergent memristive electronic devices, integrated photonics, and optical metamaterials.[80,170] Chalcogenide compounds are compositionally tunable, through combinatorial high throughput stoichiometric engineering techniques, to have a wide range of properties from the UV – visible to the mid-infrared spectral range; chalcogenides exhibit photoconduction, exceptional infrared transparency, high optical non-linearity, plasmonic, epsilon-near-zero, and high refractive index dielectric properties.[76,188] Specifically, by applying short optical or electrical pulses, phase change alloys such as Ge:Sb:Te (GST) can be switched in a reversible and non-volatile fashion between two opto-electronically distinct phases: a covalently bonded amorphous phase and a resonantly bonded crystalline phase. Transitioning from the crystalline to the amorphous phase constitutes a melt-quench process, initiated by a short duration high intensity excitation to momentarily raise the temperature above the material melting point, while the reverse transition requires an annealing process involving a longer duration low intensity excitation to hold the temperature above the glass transition temperature (lower than melting point). The versatile nature associated with phase change chalcogenides, together with its compatibility with existing complementary metal oxide (CMOS) fabrication processes have facilitated a wide range of active tunable nanophotonic metamaterial demonstrations including all-optical switching, polarization modulation, wavefront manipulation including beam – steering, and multispectral imaging.[189,190]

While the last decade has seen researchers concentrate mostly on proof-of-principle device demonstrations that enable the incorporation of phase change into the metamaterial architecture, the ensuing decade is inevitably concerned with designing devices that serve specific industrial applications with well-defined operational parameters. These include synaptic weights for photonic hardware neural nets in emerging neuromorphic processors and accelerators, temperature tolerant silicon photonic modulators with built-in memory functionality, addressable adaptive metasurfaces for smart cameras and sensors as well as local control of emission for quantum optics applications. While phase change chalcogenide semiconductors have been used in memory applications where requirements in repeated cycling (endurance) of

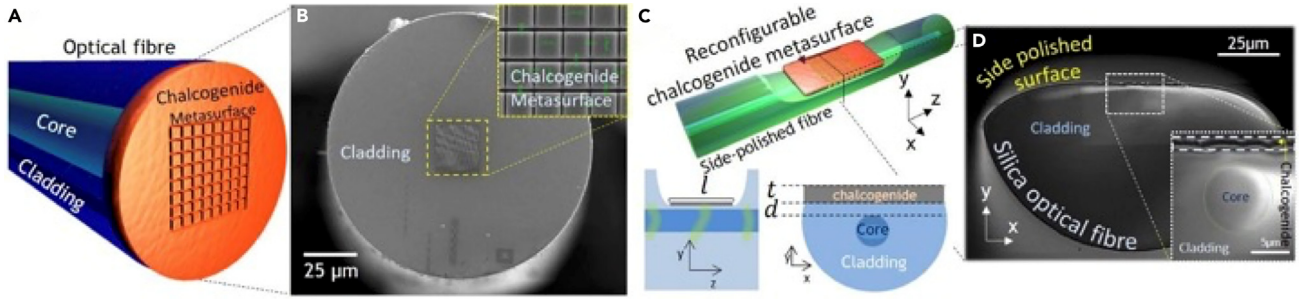

Figure 13. Integration and packaging of phase change metasurfaces

(A–D) Shows schematic and scanning electron microscopy of metadevices fabricated on (a, b) tip and (c, d) side of optical fiber, Adapted from.[191,192]

such devices is lower in comparison with applications that are currently being explored for phase change nanophotonics where in the context of signal modulation in telecommunication networks or synaptic weights in neuromorphic computing, switching on the order of $>10^{12}$ cycles are desirable. Therefore, exploring various switching protocols and mechanisms in conjunction with more complex device architectures that attempt to confine and reduce elemental migration in phase change layers has become a global effort that will lead to major reductions in the drift and noise associated with repeated switching events while enhancing the cyclability limit of various alloys. In most traditional phase change metamaterial and metasurfaces demonstrated thus far, due to the larger lateral footprint of such devices arising from their reliance on collective resonances in arrays of metamolecules, the challenge in low noise and drift, endurance cycling is compounded as transitions over relatively large micron-scale lateral areas is typically pursued using microheaters as compared to the small nanoscale vias used in electronic PCRAM devices. While the microheater approach provides favorable spatially uniform phase transitions over large lateral areas, it requires high power consumption and the incorporation of lossy metallic heaters, if fast switching is desirable. Metamaterial device architectures that take advantage of filamentation as in PCRAM rather than large area microheater based switching should yield much lower power consumptions and higher endurance that may require a major reconsideration of device architectures going forward. In the coming decades, more emphasis will start to be placed on packaging and integration of the developed devices into emerging computing and telecommunication networks reliant upon optical fiber or waveguide architectures[191] (Figure 13). While germanium antimony telluride (GST) has been traditionally favored, due to its inherent losses across visible/telecommunication frequencies, there is an ongoing global search for new alloys with more favorable insertion losses across commercially important spectral bands. This is also due to the patenting of new alloys becoming a financially lucrative endeavor. More recently the identification of selenium and sulfur-based alloys (e.g., GSST, SbS or SbSe) with lower optical losses has seen widespread adoption.[9–11,145] However, many important aspects of their performance such as switching speed limits, endurance cycling, grain sizes and chemical/environmental stability are yet to be fully understood and remain justifiably active areas of research.

In the quest for a low optical loss, fast switching alloy with universal endurance, the wide adoption of high throughput stoichiometric engineering techniques for the identification of precise compositions that exhibit low loss and favorable switching dynamics is essential in accelerating advances on this front.[188] On this front, several new alloys have recently been introduced with widespread adoption that present more favorable optical properties across visible and near infrared wavelengths, although further characterization of switching limits and endurance on these alloys is a necessity going forward (Figure 14). Furthermore, this should be extended to exploring not just tuning of chemical composition but also exploring bottom-up growth techniques that enable controlling not just the thickness but the internal morphology of phase change films. This can lead to the growth of phase change films and metasurfaces with tunable optical properties and high endurance without changing chemical composition. Switching dynamics, modulation contrasts, drift and endurance are a strong function of not just the material platform, but also the device architecture in phase change chalcogenide metasurfaces.[184,193] Therefore, aside from the need to develop mass-manufacturable fabrication and packaging techniques, there is a necessity to develop precise theoretical and simulation frameworks

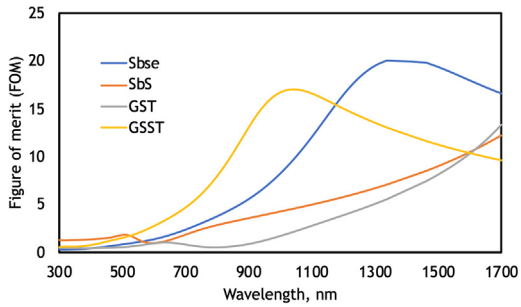

Figure 14. Visible and near infrared dispersion of figure of merit defined for a reconfigurable phase change nanophotonic medium (FOM = $\frac{n_a^3 \Delta n}{k_c}$), where n_a is refractive index of amorphous phase and k_c extinction coefficient of the lossy crystalline phase

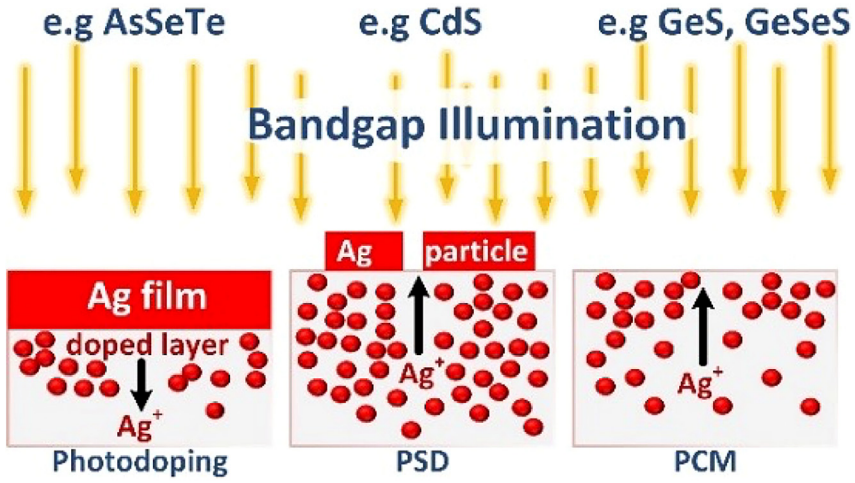

Figure 15. Comparison of different forms of photo-ionic movement possible in various chalcogenides

It illustrates a comparison of the Ag photodoping, Photo-induced surface deposition (PSD) and photo-induced chemical modification (PCM) phenomena.

that couple thermal, optical, and electronic physics for precise design of the temporal switching dynamics of such devices. The development of an end-to-end PDK for standardized widespread development of phase change metasurface based technologies is a global necessity that will need to be addressed by academic and/or commercial entities to enable mass-production and adoption of these technologies.

One of the major points of instability in phase change metasurfaces is the melt-quench transition that is required as part of a full phase change cycle. Avoiding this transition will yield higher endurance devices with lower drift going forward. On this road, the chalcogenide alloys also have other non-volatile transitions ripe for exploration as alternatives to phase change.[194] For instance, A severely overlooked property of metal doped amorphous chalcogenide semiconductors (MdACs), particularly certain sulfides and selenides, is that they exhibit directional photo-induced long-range movement of their constituent metal ions when exposed to light with a photon energy equivalent/higher than the optical band gap of the chalcogenide host. This "photo-ionic" movement results in substantial and non-volatile changes of material properties (refractive index and conductivity) at the nanoscale facilitating robust, low power, non-binary dynamic modulation of light[195] (Figure 15). Therefore, exploration and utilization of such alternative non-volatile effects that operate without the need for a power-intensive and destabilizing melt-quench process inherent to phase change should pave the way to higher endurance device platforms.

Chalcogenide phase change metamaterials and metasurfaces have become an essential part of the nanophotonic technology toolkit going forward, their considered design can enable a new generation of adaptive optoelectronic devices with tunable responses and built-in memory functionality. The rapid advancements in materials engineering fueled through more sophisticated stoichiometric engineering and bottom-up growth techniques coupled with Multiphysics modeling and simulation platforms that enable integration of these devices with mature global photonic platforms such as optical fibers and waveguides will lead to the establishment of a uniquely important device family for a myriad of optoelectronic applications going forward.

Engineering multi-material solutions for phase change materials-based integrated photonics by M.K., K.A.R.

The reversible switching property of PCMs has opened the way toward next generation memory applications such as phase-change random access memory. More recently due to the development of novel compositions aimed to reduce optical loss while maintaining high contrast switching attributes, PCMs have become viable options in the field of integrated photonic applications. In such an application, the PCM platform offers the opportunity to arbitrarily control light-matter interactions such as transmission, reflection, and beam steering. Ge-Sb-Te (GST), the most well-known, traditional PCM exhibits a low figure of merit ($\Delta n/\Delta k$) for such integrated photonic applications due to a high optical loss upon its phase change process. This has necessitated the development of new PCM compositions which can be manufactured with high quality and fidelity. Recently, alternative compositions based on Ge-Sb-Se-Te and Sb-Se have been demonstrated to be competitive candidates which can mitigate this high optical loss challenge, while still exhibiting a large refractive index contrast.[9–11,73–75,196] Meanwhile, lingering issues such as cycling degradation and low quenching speed of both traditional and alternative PCMs have been a bottleneck limiting their acceptance in mainstream PCM platforms. Here, we summarize key strategies demonstrated by various researchers to date and suggest novel approaches in material chemistry, optical properties, and multi-material processing interactions that exhibit promise toward the circumvention of these known issues.

Cycling degradation

While the Sb-Se system has an ultra-low optical loss in both glassy and crystalline states over the telecommunication frequency range,[196] its utilization as PCMs has been reported to undergo a degradation issue upon multiple cycling. Sb-Se system's phase diagram indicates that a slight deviation from the stoichiometry (i.e., 60 at% of Se) can easily form undesirable secondary phases, leading to a change in the conductivity of the

PCM and potentially affecting its cycling performance.[197] This phenomenon is exemplified in recent works by Delaney et al., where Mach-Zehnder interferometer structures based on Sb-Se as an example of PCM-based platforms suffer structural damage that initiates typically at the corner of the active layer of Sb-Se, thereby limiting cycling durability to ~350 cycles.[2,145] Here, the degradation of the cycling performance is attributed to capping layers, often used as part of PCM-based structures. In this configuration, capping layer interfaces typically have a much lower conductivity, limiting a necessary heat dissipation route. Hence, an increase in local temperature leads to the formation of voids and local non-stoichiometry, thereby ultimately causing cycling inconsistency. A possible strategy to mitigate the issue suggested in various studies is to spatially modulate pulse power applied to the PCM region such that a region prone to damage can be stimulated to a lesser degree. The creation of such local non-stoichiometry within PCM-based structures has been also observed in Ge-Sb-Te-based systems.[198] Under electric pulse activation, Sb and Te can exhibit electromigration in opposite directions. Since Sb is observed to move faster than Te, such cross electromigration can eventually lead to void creation and local non-stoichiometry. To mitigate this issue, a two-way approach is employed in.[145] First, the polarity of the electric pulse is reversed so that those spatially displaced atoms migrate back and fill the void. Second, by capping a PCM region with a metallic surfactant layer, a conductive channel can be created even in the presence of voids which otherwise make resistance go higher. In summary, the abilities to spatially modulate pulse power, reverse pulse polarity, and vary capping layers such as the use of metallic layers are three key methods that have been demonstrated to alleviate such a lingering degradation issue within PCMs.

Quenching kinetics

The ability for PCMs to be rapidly converted from a crystalline state to a glassy state is one of key metrics that defines switching performance. This phase transition rate, which allows rapid cooling from the melted media to allow formation of a disordered, glassy state, has been considered a challenge for key candidate PCMs. Here, the reorganization (diffusivity) of constituent atoms dictates the quenching kinetics. A recent computational study on the self-diffusivity of Sb_2Te_3 as a candidate for single-phase PCMs is relevant,[199] due to its structural similarity to that of Sb_2Se_3 and same constituent elements existing in Ge-Sb-Se-Te-based PCMs. In the study, the ab-initio molecular dynamics simulation is employed to estimate the evolution of Sb_2Te_3's time-dependent mean-squared atomic displacements as a function of temperature with an ultrafast cooling rate (i.e., quenching). As an example, the melting/cooling time + temperature of this system, 618°C over a duration of 100ps (typical switching time observed with other PCMs), corresponds to a self-diffusivity of the material system on the order of ~6.56 Å and is expected to be lower with decreasing temperature as quenching proceeds. This value is just slightly greater than average nearest-neighbor nearest neighbor distances of Sb-Sb: 3.26 Å, Sb-Te: 3.85 Å, and Te-Te: 3.16 Å,[8] leaving room for kinetic improvement, thus necessitating the further improvement of candidate PCM system and their neighboring platform materials.

New approaches to kinetic improvement

While the aforementioned low-loss candidate PCMs in key infrared spectral window provide a unique alternative to the more lossy traditional Ge-Sb-Te, their switching time, defined as the duration of time to crystallize with an applied heating pulse and quench via a rapid cooling of the melted phase, is slower as compared to those of other conventional PCMs. This limits, as of this time, their application as ultrafast data storages and integrated photonic platforms. The key bottleneck for the slow switching rate is the quenching step which employs amorphization through melting followed by rapid quenching. Here, the kinetics of melting and subsequent rapid quenching is largely dictated by the PCM's melting temperature and thermal conductivity, respectively. Specifically, a lower melting temperature facilitates the solid-to-liquid phase transition while a higher thermal conductivity enables better heat extraction allowing a higher quenching rate. Meanwhile, as the number of constituent elements increases in composite alloys, their liquidus temperature at/near the eutectic compositions has been reported to be correspondingly suppressed, indicating that the melting temperature of a PCM would decrease as more elements are added into the system. Efforts to this challenge are ongoing, where elemental additions could induce significant configurational entropy via random population of atoms on one type of lattice sites in the crystalline phase, thereby preventing phase separation and stabilizing a eutectic phase. This approach employing compositional mixing will enable alternative candidates based on Ge-Sb-Se-Te and Sb-Se as well as their variants with additional elements to be evaluated with the goal of lowering the energy barrier for the atomic reorganization, facilitating the PCMs' switching. While chalcogenide-based PCMs inherently have low thermal conductivities, we envision that quenching can be enhanced by making them into low-dimensional nanostructures. Such strategies, specifically, meta-layers or conformally coated layers on substrates with complex surface topography, will exhibit surface-to-volume ratios greater than that of a bulk counterpart. These structures will allow pre-existing heat within PCMs to efficiently drain off into neighboring materials, further enhancing performance.

Phase change materials for electro-thermal conversion and storage by H.Y., X.C.

Depending on the scenario requirements, energy conversion and storage are essential for practical energy utilization. Advanced functional electric-driven PCMs can convert electrical energy into thermal energy, thus playing an important role in sustainable energy utilization. Recently, PCM-based electro-thermal conversion and storage technology have shown great potential in the thermal management of electronic devices, power vehicles, human body, and off-peak power storage systems.[200,201] Due to the inherent insulating nature of pristine PCMs, PCMs are usually encapsulated to trigger their electro-thermal conversion and storage using electrically conductive supporting scaffolds.[202,203] The main electrically conductive supporting scaffolds include carbon nanotubes (CNTs), graphene and its derivatives, biomass-derived carbon, metal-organic frameworks (MOFs)-derived carbon, graphite, highly graphitized carbon, and MXene (Figure 16). In addition to electrical conductivity, thermal conductivity is also an important factor affecting the electro-thermal conversion and storage capacity of composite PCMs.

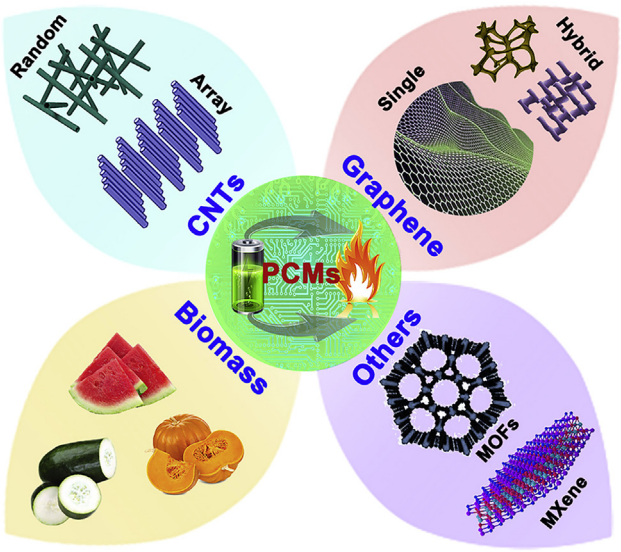

Figure 16. Main conductive supporting scaffolds for electric-driven composite PCMs
Adapted with permission from.[203,204]

PCM-based energy conversion and storage systems are promising to address the high-energy consumption problem of fossil fuels and intermittency problem of renewable sources due to the storage and release of large amounts of latent heat through phase transition processes with small temperature changes. However, the inherent low thermal conductivity (0.2–0.3 W/m·K) and electrical conductivity (10^{-14}-10^{-13} S/m) of pristine PCMs makes them impossible to achieve electro-thermal conversion alone.[9–11] Intriguingly, the introduction of highly thermally and electrically conductive supporting scaffolds endows PCMs with electro-thermal conversion and storage function. The fundamental mechanism of electro-thermal conversion and storage of composite PCMs is as follows. When the conductive composite PCMs are connected to the circuit, joule heat is generated due to the collision between moving electrons and other groups or molecules.[9–11] In the initial stage, the temperature of composite PCMs rises sharply by the generated joule heat until the melting point of composite PCMs is reached. At this time, PCM molecules begin to undergo an order-disorder phase transition, and the thermal energy converted from electrical energy is stored in the form of latent heat. Generally, a higher applied voltage will lead to a higher electro-thermal conversion and storage efficiency. It is worth noting that the electro-thermal conversion process of composite PCMs cannot be triggered below the critical driving voltage. Lower operating voltage and higher electro-thermal conversion and storage efficiency are two key metrics pursued simultaneously.

Table 3 summarizes various composite PCMs for electro-thermal conversion and storage. Carbon materials (e.g., graphite,[205] carbon nanotube,[206] graphene,[208] carbon fiber,[59–62] biomass derived carbon[212]) are conventional electrically conductive supporting scaffolds for joule heating of PCMs. Except these highly conductive fillers, some novel conductive materials have also been utilized for electro-thermal conversion and storage of PCMs recently, such as MXene[104,105] and MOF-derived carbon.[207] In general, hybrid conductive fillers are advantageous to the construction of highly continuous thermally and electrically conductive channels.[203,204] For instance, our group[207] prepared a CNT/porous carbon hybrid to encapsulate octadecane via high-temperature carbonization of ZIF-67@IRMOF-3 with core-shell structure. Compared with single porous carbon, ZIF-67@IRMOF-3 derived CNT-penetrated porous carbon exhibited a more denser 3D conductive network. Abundant CNTs facilitated the interfacial interaction between carbon support and octadecane, enabling fast thermal transformation. Resultantly, CNT/porous carbon hybrid-based composite PCMs achieved a record-high electro-thermal conversion and storage efficiency of 94.5% at an ultralow critical triggering voltage of 1.1 V, showing great application potential in thermal management of electronic devices.

Although the introduction of highly thermally and electrically conductive supporting scaffolds have greatly enhanced the thermal and electric response capabilities of PCMs, there are still some challenges that hinder the large-scale practical applications of composite PCMs. Conventionally, a high proportion (20–40 wt. %) of conductive fillers is usually required to be incorporated into PCMs to obtain high thermal and electrical conductivities.[214] However, a high proportion of conductive fillers will inevitably reduce the loading content of PCMs, thereby reducing the thermal storage capacity of composite PCMs due to their inactive characteristics. Furthermore, random conductive fillers tend to aggregate after undergoing multiple thermal cycles, eventually leading to partial separation of fillers from PCMs. Consequently, the thermal and electrical conductivities of composite PCMs greatly decline due to the discontinuous contact between conductive fillers and PCMs. Some conductive fillers exposed on the surface of composite PCMs inevitably increase convection heat dissipation at the solid-air interface, which is not conducive to achieving high energy conversion and storage efficiency at a low voltage.[207] Another challenge is the structural brittleness and rigidity of most composite PCMs, which is caused by the fragility of the supporting scaffolds. It is also noteworthy that the flexibility of some reported flexible composite PCMs will decline sharply or even disappear completely in the crystalline state of PCMs. The insufficient

Table 3. Summary of composite PCMs for electro-thermal conversion and storage

Functional fillers	PCMs	Melting point (°C)	Melting enthalpy (J/g)	Thermal conductivity (W/m·K)	Electrical conductivity (S/m)	Input voltage (V)	Conversion efficiency (%)	Reference
Graphite	Pentaerythritol	186.6	292.3	33.5	323	0.34	92.7	Li et al., 2021[205]
Graphite foam	Paraffin	51.0	209.2	1.38	–	5.0	74.6	Liu et al., 2022a, 2022b, 2022c, 2022d[59–62]
CNT	n-Eicosane	43.0	217.3	–	–	1.3	74.7	Liu et al., 2013[206]
CNT@porous carbon	Octadecane	31.9	135.9	–	526.3	1.1	94.5	Li et al., 2020[207]
Graphene	PEG10000	47.6	118.7	–	–	1.5	94.0	Kou et al., 2021[208]
Graphene aerogel	Paraffin	47.8	193.7	2.99	2.99	1.5	50.5	Li et al., 2016[209]
Graphene/cellulose	PEG6000	67.6	182.6	1.03	–	10.0	–	Wei et al., 2019[210]
Graphene/cellulose	Paraffin	46.7	147.9	1.42	3.38	5.0	–	Xue et al., 2020[211]
SiO_2/carbon fiber	Paraffin	61.2	183.8	0.73	4.95	3.0	82.2	Liu et al., 2022a, 2022b, 2022c, 2022d[59–62]
Carbon fiber	Paraffin	39.22	182.2	0.53	19.6	3.0	81.1	Umair et al., 2020[212]
rGo/BN	PEG10000	59.5	164.1	1.06	–	7.0	87.9	Yang et al., 2020a, 2020b, 2020c[100–102]
MXene/porous carbon	Paraffin	40.0	215.7	–	9.62	8.0	–	Cao et al., 2022a, 2022b[104,105]
Copper foam	PEG6000	63.6	152.5	0.33	30.81	2.25	85.6	Xiao et al., 2021[213]

flexibility of composite PCMs often results in difficult fixation in a narrow space or non-intimate contact between composite PCMs and target objects (e.g., lithium batteries, smartphones, chips, skin).[215]

Compared with microencapsulation, 3D stabilized interpenetrating filler scaffolds (e.g., aerogel, foam, sponge, fiber) require a smaller proportion to achieve highly thermal and electrical conductivities and high energy storage density.[216,217] The conductive pathways constructed by 3D filler scaffolds are affected by a combination of pore structure, spatial arrangement, and degree of orientation. The rational combination of these factors plays a significant role in reducing the electric and thermal resistance to enhance the electro-thermal conversion and storage capability of composite PCMs. Compared with random structures, highly array-oriented 3D scaffolds with regular pore structure and high specific surface area are more conducive to improving the electro-thermal conversion and storage capability of composite PCMs. This is because array-oriented 3D scaffolds can provide sufficient active interfaces for the crystallization of PCM molecules and establish continuously interpenetrating electrical and thermal conduction channels to reduce interface resistance and can adapt to the volume expansion during the phase transition process to guarantee the uniform distribution of PCM molecules.[216,218] The fabrication methods of 3D array-oriented scaffolds for electric-driven composite PCMs mainly include chemical vapor deposition,[206] high-temperature carbonization,[209] freeze casting,[210] ice-templated method,[211] etc. In addition, selecting flexible supporting scaffolds with good thermal and electrical conductivities for PCMs is one of the most common approaches to endow flexible composite PCMs with high electro-thermal conversion and storage capability. There are usually two strategies to prepare flexible conductive supporting scaffolds. One strategy is to directly assemble conductive fillers into flexible scaffolds through various methods, such as high-temperature carbonization,[59–62] chemical polymerization,[208] and electro-spinning.[219] Another strategy is to choose flexible porous scaffolds as templates to grow conductive fillers.[213] These practices provide constructive guidance for the development of high-performance electric-driven PCMs.

Advanced functional electric-driven PCMs have broadened the application range of PCMs from conventional thermal energy storage to thermal management of electronic devices and the human body. Herein, we review the recent advances in electric-driven PCMs and highlight the current and future challenges. In general, highly ordered orientation and flexible supporting scaffolds are more favorable for the practical applications of electric-driven PCMs. While electric-driven PCMs have made some progress, there is still large room for improvement. Balancing low voltage driving and high energy conversion efficiency is a difficulty in future research. The microscopic mechanism of electro-thermal conversion of PCMs is still unclear, requiring in-depth and systematic revealing. The influences of filler-filler interface and filler-matrix interface on the thermophysical properties of composite PCMs have not been well studied. It is necessary to establish a standardized test method to evaluate the electro-thermal conversion and storage efficiency of composite PCMs.

CONCLUSIONS

The advancement of high-performance broadband PCMs will bring about new innovations and applications, as well as have a significant impact on thermal energy storage, thermal management, and reconfigurable photonics. The stable and power-efficient tuning and

reconfigurability across a wide spectral band, ultrafast switching speed, and zero-energy stable phase change state of PCMs make them a unique solution. The optical and electronic properties can be quickly altered by stimulation with optical or electrical pulses, making PCMs a versatile material with a range of potential applications.

The roadmap has discussed advancements in two main categories of applications: reconfigurable nanophotonics and thermal energy management, using different types of PCMs.

For reconfigurable nanophotonics employing chalcogenide PCMs, several crucial challenges and avenues for research advancement warrant attention. Foremost among these challenges is the imperative to enhance the energy efficiency of these materials. While chalcogenide PCMs hold the potential for versatile operation through diverse material configurations, they confront critical issues related to energy efficiency and optical losses. The optimization of these materials is imperative to curtail energy consumption and bolster overall performance. Another challenge lies in overcoming the technical complexities associated with dynamic switching and reconfigurability in the long wavelength region. The larger feature size of these platforms in this context can impose limitations on the speed and precision of switching. Conversely, in shorter wavelength regions such as UV and visible light, optical loss emerges as the primary restraining factor. Pioneering efforts are required to devise strategies for minimizing optical loss in these materials, thus elevating the overall performance of the system.

For thermal energy storage applications, PCMs have the potential to play a pivotal role in advancing the field. Specifically, advanced functional electric-driven PCMs have expanded the scope of PCM applications beyond conventional thermal energy storage to encompass thermal management for electronic devices and even human comfort. The highly ordered orientation and adaptable supporting structures make electric-driven PCMs well-suited for practical applications. While electric-driven PCMs have made notable strides, substantial room for improvement remains. A key challenge is striking a balance between low-voltage operation and high energy conversion efficiency: a task that presents difficulties in future research. In essence, researchers must seek methods to minimize the voltage necessary for driving the phase change process while simultaneously maximizing the storage and release of energy through this process. The subsequent objective is to identify materials capable of being charged and discharged with low voltage, all while maintaining a high level of heat energy conversion efficiency. This pursuit is intricate, as enhancing energy conversion efficiency often necessitates higher voltage, potentially at odds with the goal of reducing voltage. Overall, the development of electric-driven PCMs holds significant potential for further improvement, and it is poised to remain an active area of research in the foreseeable future.

Recent strides in fabrication techniques and the embrace of innovative design principles have markedly alleviated the constraints on PCM-based devices in recent years. This has translated into enhanced energy efficiency and reduced optical losses, ultimately yielding more practical and dependable PCM-based devices. The realm of phase change photonics is poised to remain a focal point of research attention, given its immense potential to reshape the landscape of next-generation technologies. The merging of static photonics with dynamic, flexible photonics introduces on-demand, adaptive capabilities, marking the dawn of a new era characterized by enhanced flexibility and performance in photonic systems. Moreover, the integration of PCMs into neuromorphic computing and artificial intelligence holds the promise of significantly augmenting the speed and efficiency of these systems.

In conclusion, the development of PCMs-based devices is a rapidly evolving field with significant potential for revolutionizing a wide range of technologies. Further research and development in this area is expected to lead to even greater advancements in the coming years.

ACKNOWLEDGMENTS

The authors Y.M.S., H-H.J., J.H.K., Y.J.Y., and Y.L. acknowledge the funding support from National Research Foundation of Korea (NRF) funded by the Ministry of Science and ICT. (NRF-2021M3H4A1A04086357 and NRF-2022M3C1A3081312).

The authors M.W. and M.J.M. acknowledge funding from the Deutsche Forschungsgemeinschaft (DFG) via the collaborative research center Nanoswitches (SFB 917) and from the Federal Ministry of Education and Research (BMBF, Germany) in the project NeuroSys (03ZU1106BA).

The authors P.P. and R.S. acknowledge the funding support from National Research Foundation (NRF) Singapore under CRP program, Grant No: NRF-CRP23-2019-0005.

The authors K.V.S. and J. T. acknowledge the funding support from the National Research Foundation Singapore under CRP program (Grant No. NRF-CRP26-2021-0004) and A*STAR (Agency for Science, Technology and Research) under AME IRG Program (Grant No. A2083c0058).

The author Z. T. acknowledges funding support from the National Natural Science Foundation of China (No. 62235013), Tianjin Municipal Fund for Distinguished Young Scholars (Grant No. 20JCJQJC00190), and Key Fund of Shenzhen Natural Science Foundation (Grant No. JCYJ20200109150212515).

The author M. L. acknowledges the support from the European Union's Horizon 2020 research and innovation program Grant No 899598 - PHEMTRONICS.

The authors C-C.P., B.M., T.G., and J.H. cordially acknowledge funding support provided by the National Science Foundation under award number 2132929 and the Draper Scholar Program.

Authors Ar.M., acknowledge the research funded by National Science Foundation (NSF-2003509), ONR-YIP Award, DARPA-AFA Award, NASA-STTR Award 80NSSC22PA980 and Intel.

The authors Av. M., Y.C., A.S.A., V.B. and B.G. acknowledge the funding by University of Alberta Future Energy Systems Institute, Alberta Innovates and Natural Sciences and Engineering Research Council of Canada.

The authors H. T., Y. W., Q.H., Y.L., Z.L., and X.M. acknowledge the support from Hubei Engineering Research Center on Microelectronics.

The authors M.K., K.A.R. acknowledge funding support provided by the National Science Foundation under award number 2132929.

The authors would like to deeply acknowledge efforts of iScience editor Dr. Kanudha Sharda, who invited submissions and complied the special issue on phase change and all-dielectric materials for photonics (https://www.sciencedirect.com/journal/iscience/special-issue/10J7ZM3QGQF) in addition to collating each section of this article. Dr. Sharda coordinated, edited technical writing of the text, and provided valuable feedback to all the contributing authors of this manuscript during all stages.

DECLARATION OF INTERESTS

R.S. is a consulting academic editor at iScience.

REFERENCES

1. Ko, J.H., Yoo, Y.J., Lee, Y., Jeong, H.-H., and Song, Y.M. (2022). A review of tunable photonics: Optically active materials and applications from visible to terahertz. iScience104727.
2. Delaney, M., Zeimpekis, I., Lawson, D., Hewak, D.W., and Muskens, O.L. (2020). A New Family of Ultralow Loss Reversible Phase-Change Materials for Photonic Integrated Circuits: Sb2S3 and Sb2Se3. Adv. Funct. Mater. *30*, 2002447.
3. Derkaoui, I., Khenfouch, M., Benkhali, M., and Rezzouk, A. (2019). VO2 thin films for smart windows: Numerical study of the optical properties and performance improvement. In Journal of Physics: Conference Series, IOP Publishing.
4. Julian, M.N., Williams, C., Borg, S., Bartram, S., and Kim, H.J. (2020). Reversible optical tuning of GeSbTe phase-change metasurface spectral filters for mid-wave infrared imaging. Optica *7*, 746–754.
5. Liu, H., Dong, W., Wang, H., Lu, L., Ruan, Q., Tan, Y.S., Simpson, R.E., and Yang, J.K.W. (2020). Rewritable color nanoprints in antimony trisulfide films. Sci. Adv. *6*, eabb7171.
6. Makino, K., Kato, K., Saito, Y., Fons, P., Kolobov, A.V., Tominaga, J., Nakano, T., and Nakajima, M. (2019). Terahertz spectroscopic characterization of Ge 2 Sb 2 Te 5 phase change materials for photonics applications. J. Mater. Chem. C Mater. *7*, 8209–8215.
7. Tian, X., and Li, Z.-Y. (2018). An optically-triggered switchable mid-infrared perfect absorber based on phase-change material of vanadium dioxide. Plasmonics *13*, 1393–1402.
8. Van Bilzen, B., Homm, P., Dillemans, L., Su, C.-Y., Menghini, M., Sousa, M., Marchiori, C., Zhang, L., Seo, J.W., and Locquet, J.-P. (2015). Production of VO2 thin films through post-deposition annealing of V2O3 and VOx films. Thin Solid Films *591*, 143–148.
9. Zhang, H., Zhou, L., Lu, L., Xu, J., Wang, N., Hu, H., Rahman, B.M.A., Zhou, Z., and Chen, J. (2019a). Miniature Multilevel Optical Memristive Switch Using Phase Change Material. ACS Photonics *6*, 2205–2212.
10. Zhang, Y., Chou, J.B., Li, J., Li, H., Du, Q., Yadav, A., Zhou, S., Shalaginov, M.Y., Fang, Z., Zhong, H., et al. (2019b). Broadband transparent optical phase change materials for high-performance nonvolatile photonics. Nat. Commun. *10*, 4279.
11. Zhang, Y., Umair, M.M., Zhang, S., and Tang, B. (2019c). Phase change materials for electron-triggered energy conversion and storage: a review. J. Mater. Chem. A Mater. *7*, 22218–22228.
12. Zheng, J., Khanolkar, A., Xu, P., Colburn, S., Deshmukh, S., Myers, J., Frantz, J., Pop, E., Hendrickson, J., Doylend, J., et al. (2018). GST-on-silicon hybrid nanophotonic integrated circuits: a non-volatile quasi-continuously reprogrammable platform. Opt. Mater. Express *8*, 1551–1561.
13. Ko, J.H., Yoo, Y.J., Kim, Y.J., Lee, S.S., and Song, Y.M. (2020). Flexible, large-area covert polarization display based on ultrathin lossy nanocolumns on a metal film. Adv. Funct. Mater. *30*, 1908592.
14. Yoo, Y.J., Ko, J.H., Kim, W.-G., Kim, Y.J., Kong, D.-J., Kim, S., Oh, J.-W., and Song, Y.M. (2020). Dual-mode colorimetric sensor based on ultrathin resonating facilitator capable of nanometer-thick virus detection for environment monitoring. ACS Appl. Nano Mater. *3*, 6636–6644.
15. Yoo, Y.J., Ko, J.H., Lee, G.J., Kang, J., Kim, M.S., Stanciu, S.G., Jeong, H.H., Kim, D.H., and Song, Y.M. (2022). Gires–Tournois Immunoassay Platform for Label-Free Bright-Field Imaging and Facile Quantification of Bioparticles. Adv. Mater. *34*, 2110003.
16. Ríos, C., Hosseini, P., Taylor, R.A., and Bhaskaran, H. (2016). Color depth modulation and resolution in phase-change material nanodisplays. Adv. Mater. *28*, 4720–4726.
17. Hosseini, P., Wright, C.D., and Bhaskaran, H. (2014). An optoelectronic framework enabled by low-dimensional phase-change films. Nature *511*, 206–211.
18. Qu, Y., Li, Q., Cai, L., Pan, M., Ghosh, P., Du, K., and Qiu, M. (2018). Thermal camouflage based on the phase-changing material GST. Light Sci. Appl. *7*, 26.
19. Ríos, C., Stegmaier, M., Hosseini, P., Wang, D., Scherer, T., Wright, C.D., Bhaskaran, H., and Pernice, W.H.P. (2015). Integrated all-photonic non-volatile multi-level memory. Nat. Photonics *9*, 725–732.
20. Wang, Y., Landreman, P., Schoen, D., Okabe, K., Marshall, A., Celano, U., Wong, H.S.P., Park, J., and Brongersma, M.L. (2021a). Electrical tuning of phase-change antennas and metasurfaces. Nat. Nanotechnol. *16*, 667–672.
21. Wang, Y., Ning, J., Lu, L., Bosman, M., and Simpson, R.E. (2021b). A scheme for simulating multi-level phase change photonics materials. npj Comput. Mater. *7*, 183.
22. Pitchappa, P., Kumar, A., Prakash, S., Jani, H., Venkatesan, T., and Singh, R. (2019). Chalcogenide Phase Change Material for Active Terahertz Photonics. Adv. Mater. *31*, 1808157.
23. Peng, J., Jeong, H.-H., Lin, Q., Cormier, S., Liang, H.-L., De Volder, M.F.L., Vignolini, S., and Baumberg, J.J. (2019). Scalable electrochromic nanopixels using plasmonics. Sci. Adv. *5*, eaaw2205.
24. Ovshinsky, S.R. (1968). Reversible Electrical Switching Phenomena in Disordered Structures. Phys. Rev. Lett. *21*, 1450–1453.
25. Feinleib, J., deNeufville, J., Moss, S.C., and Ovshinsky, S.R. (1971). RAPID REVERSIBLE LIGHT-INDUCED CRYSTALLIZATION OF AMORPHOUS SEMICONDUCTORS. Appl. Phys. Lett. *18*, 254–257.
26. Nandakumar, S.R., Le Gallo, M., Boybat, I., Rajendran, B., Sebastian, A., and Eleftheriou, E. (2018). A phase-change memory model for neuromorphic computing. J. Appl. Phys. *124*, 152135.
27. Zhang, Q., Zhang, Y., Li, J., Soref, R., Gu, T., and Hu, J. (2018). Broadband nonvolatile photonic switching based on optical phase change materials: beyond the classical figure-of-merit. Opt. Lett. *43*, 94–97.
28. Carrillo, S.G.-C., Trimby, L., Au, Y.-Y., Nagareddy, V.K., Rodriguez-Hernandez, G., Hosseini, P., Ríos, C., Bhaskaran, H., and Wright, C.D. (2019). A Nonvolatile Phase-Change Metamaterial Color Display. Adv. Opt. Mater. *7*, 1801782.

29. Wuttig, M., Deringer, V.L., Gonze, X., Bichara, C., and Raty, J.-Y. (2018). Incipient Metals: Functional Materials with a Unique Bonding Mechanism. Adv. Mater. *30*, 1803777.
30. Wuttig, M., Schön, C.-F., Lötfering, J., Golub, P., Gatti, C., and Raty, J.-Y. (2022). Revisiting the Nature of Chemical Bonding in Chalcogenides to Explain and Design their Properties. Adv. Mater. *35*, 2208485.
31. Raty, J.-Y., Schumacher, M., Golub, P., Deringer, V.L., Gatti, C., and Wuttig, M. (2019). A Quantum-Mechanical Map for Bonding and Properties in Solids. Adv. Mater. *31*, 1806280.
32. Guarneri, L., Jakobs, S., von Hoegen, A., Maier, S., Xu, M., Zhu, M., Wahl, S., Teichrib, C., Zhou, Y., Cojocaru-Mirédin, O., et al. (2021). Metavalent Bonding in Crystalline Solids: How Does It Collapse? Adv. Mater. *33*, 2102356.
33. Kerres, P., Zhou, Y., Vaishnav, H., Raghuwanshi, M., Wang, J., Häser, M., Pohlmann, M., Cheng, Y., Schön, C.F., Jansen, T., et al. (2022). Scaling and Confinement in Ultrathin Chalcogenide Films as Exemplified by GeTe. Small *18*, 2201753.
34. Zhu, M., Cojocaru-Mirédin, O., Mio, A.M., Keutgen, J., Küpers, M., Yu, Y., Cho, J.-Y., Dronskowski, R., and Wuttig, M. (2018). Unique Bond Breaking in Crystalline Phase Change Materials and the Quest for Metavalent Bonding. Adv. Mater. *30*, 1706735.
35. Schön, C.F., van Bergerem, S., Mattes, C., Yadav, A., Grohe, M., Kobbelt, L., and Wuttig, M. (2022). Classification of properties and their relation to chemical bonding: Essential steps toward the inverse design of functional materials. Sci. Adv. *8*, eade0828.
36. Arora, R., Waghmare, U.V., and Rao, C.N.R. (2022). Metavalent Bonding Origins of Unusual Properties of Group IV Chalcogenides. Adv. Mater. *35*, 2208724.
37. Kooi, B.J., and Wuttig, M. (2020). Chalcogenides by Design: Functionality through Metavalent Bonding and Confinement. Adv. Mater. *32*, 1908302.
38. Müller, M.J., Yadav, A., Persch, C., Wahl, S., Hoff, F., and Wuttig, M. (2022). Tailoring Crystallization Kinetics of Chalcogenides for Photonic Applications. Advanced Electronic Materials *8*, 2100974.
39. Persch, C., Müller, M.J., Yadav, A., Pries, J., Honné, N., Kerres, P., Wei, S., Tanaka, H., Fantini, P., Varesi, E., et al. (2021). The potential of chemical bonding to design crystallization and vitrification kinetics. Nat. Commun. *12*, 4978.
40. Behrens, M., Lotnyk, A., Gerlach, J.W., Ehrhardt, M., Lorenz, P., and Rauschenbach, B. (2019). Direct Measurement of Crystal Growth Velocity in Epitaxial Phase-Change Material Thin Films. ACS Appl. Mater. Interfaces *11*, 41544–41550.
41. Rajendran, B., Sebastian, A., Schmuker, M., Srinivasa, N., and Eleftheriou, E. (2019). Low-Power Neuromorphic Hardware for Signal Processing Applications: A Review of Architectural and System-Level Design Approaches. IEEE Signal Process. Mag. *36*, 97–110.
42. Singh, A., Li, Y., Fodor, B., Makai, L., Zhou, J., Xu, H., Akey, A., Li, J., and Jaramillo, R. (2019). Near-infrared optical properties and proposed phase-change usefulness of transition metal disulfides. Appl. Phys. Lett. *115*, 161902.
43. Wuttig, M., Schoen, C.-F., Schumacher, M., Robertson, J., Golub, P., Bousquet, E., and Raty, J.-Y. (2020). Halide perovskites: third generation photovoltaic materials empowered by metavalent bonding. Preprint at arXiv. https://doi.org/10.48550/arXiv.2012.03794.
44. Maier, S., Steinberg, S., Cheng, Y., Schön, C.F., Schumacher, M., Mazzarello, R., Golub, P., Nelson, R., Cojocaru-Mirédin, O., Raty, J.-Y., and Wuttig, M. (2020). Discovering Electron-Transfer-Driven Changes in Chemical Bonding in Lead Chalcogenides (PbX, where X = Te, Se, S, O). Adv. Mater. *32*, 2005533.
45. Heßler, A., Wahl, S., Leuteritz, T., Antonopoulos, A., Stergianou, C., Schön, C.F., Naumann, L., Eicker, N., Lewin, M., Maß, T.W.W., et al. (2021). In3SbTe2 as a programmable nanophotonics material platform for the infrared. Nat. Commun. *12*, 924.
46. Ronneberger, I., Zanolli, Z., Wuttig, M., and Mazzarello, R. (2020). Changes of Structure and Bonding with Thickness in Chalcogenide Thin Films. Adv. Mater. *32*, 2001033.
47. Sámson, Z.L., MacDonald, K.F., De Angelis, F., Gholipour, B., Knight, K., Huang, C.C., Di Fabrizio, E., Hewak, D.W., and Zheludev, N.I. (2010). Metamaterial electro-optic switch of nanoscale thickness. Appl. Phys. Lett. *96*, 143105.
48. Abdollahramezani, S., Hemmatyar, O., Taghinejad, M., Taghinejad, H., Kiarashinejad, Y., Zandehshahvar, M., Fan, T., Deshmukh, S., Eftekhar, A.A., Cai, W., et al. (2021). Dynamic Hybrid Metasurfaces. Nano Lett. *21*, 1238–1245.
49. Abdollahramezani, S., Hemmatyar, O., Taghinejad, M., Taghinejad, H., Krasnok, A., Eftekhar, A.A., Teichrib, C., Deshmukh, S., El-Sayed, M.A., Pop, E., et al. (2022). Electrically driven reprogrammable phase-change metasurface reaching 80% efficiency. Nat. Commun. *13*, 1696.
50. Baranov, D.G., Xiao, Y., Nechepurenko, I.A., Krasnok, A., Alù, A., and Kats, M.A. (2019). Nanophotonic engineering of far-field thermal emitters. Nat. Mater. *18*, 920–930.
51. Karvounis, A., Gholipour, B., MacDonald, K.F., and Zheludev, N.I. (2016). All-dielectric phase-change reconfigurable metasurface. Appl. Phys. Lett. *109*, 051103.
52. Petronijevic, E., and Sibilia, C. (2016). All-optical tuning of EIT-like dielectric metasurfaces by means of chalcogenide phase change materials. Opt Express *24*, 30411–30420.
53. Chen, C., Kaj, K., Zhao, X., Huang, Y., Averitt, R.D., and Zhang, X. (2022a). On-demand terahertz surface wave generation with microelectromechanical-system-based metasurface. Optica *9*, 17–25.
54. Chen, J., Chen, X., Liu, K., Zhang, S., Cao, T., and Tian, Z. (2022b). A Thermally Switchable Bifunctional Metasurface for Broadband Polarization Conversion and Absorption Based on Phase-Change Material. Advanced Photonics Research *3*, 2100369.
55. Chen, R., Fang, Z., Fröch, J.E., Xu, P., Zheng, J., and Majumdar, A. (2022c). Broadband Nonvolatile Electrically Controlled Programmable Units in Silicon Photonics. ACS Photonics *9*, 2142–2150.
56. Chen, X., Zhang, S., Liu, K., Li, H., Xu, Y., Chen, J., Lu, Y., Wang, Q., Feng, X., Wang, K., et al. (2022d). Reconfigurable and Nonvolatile Terahertz Metadevices Based on a Phase-Change Material. ACS Photonics *9*, 1638–1646.
57. Dong, W., Qiu, Y., Zhou, X., Banas, A., Banas, K., Breese, M.B.H., Cao, T., and Simpson, R.E. (2018). Tunable Mid-Infrared Phase-Change Metasurface. Adv. Opt. Mater. *6*, 1701346.
58. Lin, Q.-W., Wong, H., Huitema, L., and Crunteanu, A. (2022). Coding Metasurfaces with Reconfiguration Capabilities Based on Optical Activation of Phase-Change Materials for Terahertz Beam Manipulations. Adv. Opt. Mater. *10*, 2101699.
59. Liu, H., Yang, G., Ji, M., Zhu, C., and Xu, J. (2022a). Phase change materials with multiple energy conversion and storage abilities based on large-scale carbon felts. Compos. Sci. Technol. *221*, 109177.
60. Liu, K., Chen, X., Lian, M., Jia, J., Su, Y., Ren, H., Zhang, S., Xu, Y., Chen, J., Tian, Z., and Cao, T. (2022b). Nonvolatile Reconfigurable Electromagnetically Induced Transparency with Terahertz Chalcogenide Metasurfaces. Laser Photon. Rev. *16*, 2100393.
61. Liu, M., Zhang, X., Liu, X., Wu, X., Ye, X., Qiao, J., Sun, Z., Zhu, X., and Huang, Z. (2022c). Multienergy-Triggered Composite Phase-Change Materials Based on Graphite Foams Synthesized from Graphite Extracted from Spent Lithium-Ion Batteries. ACS Sustain. Chem. Eng. *10*, 8051–8063.
62. Liu, Y., Qiu, Z., Ji, X., Lukashchuk, A., He, J., Riemensberger, J., Hafermann, M., Wang, R.N., Liu, J., Ronning, C., and Kippenberg, T.J. (2022d). A photonic integrated circuit–based erbium-doped amplifier. Science *376*, 1309–1313.
63. Pinaud, M., Humbert, G., Engelbrecht, S., Merlat, L., Fischer, B.M., and Crunteanu, A. (2021). Terahertz Devices Using the Optical Activation of GeTe Phase Change Materials: Toward Fully Reconfigurable Functionalities. ACS Photonics *8*, 3272–3281.
64. Qu, Y., Li, Q., Du, K., Cai, L., Lu, J., and Qiu, M. (2017). Dynamic Thermal Emission Control Based on Ultrathin Plasmonic Metamaterials Including Phase-Changing. Laser Photon. Rev. *11*, 1700091.
65. Zhu, H., Li, J., Lu, X., Shi, Q., Du, L., Zhai, Z., Zhong, S., Wang, W., Huang, W., and Zhu, L. (2022). Volatile and Nonvolatile Switching of Phase Change Material Ge2Sb2Te5 Revealed by Time-Resolved Terahertz Spectroscopy. J. Phys. Chem. Lett. *13*, 947–953.
66. Gholipour, B., Piccinotti, D., Karvounis, A., MacDonald, K.F., and Zheludev, N.I. (2019). Reconfigurable Ultraviolet and High-Energy Visible Dielectric Metamaterials. Nano Lett. *19*, 1643–1648.
67. Michel, A.-K.U., Chigrin, D.N., Maß, T.W.W., Schönauer, K., Salinga, M., Wuttig, M., and Taubner, T. (2013). Using Low-Loss Phase-Change Materials for Mid-Infrared Antenna Resonance Tuning. Nano Lett. *13*, 3470–3475.
68. Yin, X., Schäferling, M., Michel, A.-K.U., Tittl, A., Wuttig, M., Taubner, T., and Giessen, H. (2015). Active Chiral Plasmonics. Nano Lett. *15*, 4255–4260.
69. Yin, X., Steinle, T., Huang, L., Taubner, T., Wuttig, M., Zentgraf, T., and Giessen, H. (2017). Beam switching and bifocal zoom lensing using active plasmonic metasurfaces. Light Sci. Appl. *6*, e17016.

70. Shalaginov, M.Y., An, S., Zhang, Y., Yang, F., Su, P., Liberman, V., Chou, J.B., Roberts, C.M., Kang, M., Rios, C., et al. (2021). Reconfigurable all-dielectric metalens with diffraction-limited performance. Nat. Commun. *12*, 1225.
71. Forouzmand, A., and Mosallaei, H. (2018). Dynamic beam control via Mie-resonance based phase-change metasurface: a theoretical investigation. Opt Express *26*, 17948–17963.
72. Ghosh, R.R., and Dhawan, A. (2023). Low loss, broadband, and non-volatile 'directed logic operations' using phase change materials in silicon photonics. IEEE J. Quant. Electron. *59*, 1–13.
73. Zhang, Y., Fowler, C., Liang, J., Azhar, B., Shalaginov, M.Y., Deckoff-Jones, S., An, S., Chou, J.B., Roberts, C.M., Liberman, V., et al. (2021a). Electrically reconfigurable non-volatile metasurface using low-loss optical phase-change material. Nat. Nanotechnol. *16*, 661–666.
74. Zhang, Y., Ríos, C., Shalaginov, M.Y., Li, M., Majumdar, A., Gu, T., and Hu, J. (2021b). Myths and truths about optical phase change materials: A perspective. Appl. Phys. Lett. *118*, 210501.
75. Zhang, Y., Zhang, Q., Ríos, C., Shalaginov, M.Y., Chou, J.B., Roberts, C., Miller, P., Robinson, P., Liberman, V., Kang, M., et al. (2021c). Transient Tap Couplers for Wafer-Level Photonic Testing Based on Optical Phase Change Materials. ACS Photonics *8*, 1903–1908.
76. Gholipour, B., Karvounis, A., Yin, J., Soci, C., MacDonald, K.F., and Zheludev, N.I. (2018). Phase-change-driven dielectric-plasmonic transitions in chalcogenide metasurfaces. NPG Asia Mater. *10*, 533–539.
77. Kobayashi, M., Arashida, Y., Asakawa, K., Kaneshima, K., Kuwahara, M., Konishi, K., Yumoto, J., Kuwata-Gonokami, M., Takeda, J., and Katayama, I. (2023). Pulse-to-pulse ultrafast dynamics of highly photoexcited Ge2Sb2Te5 thin films. Jpn. J. Appl. Phys. *62*, 022001.
78. Raeis-Hosseini, N., and Rho, J. (2019). Dual-Functional Nanoscale Devices Using Phase-Change Materials: A Reconfigurable Perfect Absorber with Nonvolatile Resistance-Change Memory Characteristics. Appl. Sci. *9*, 564.
79. Piccinotti, D., Gholipour, B., Yao, J., Macdonald, K.F., Hayden, B.E., and Zheludev, N.I. (2018). Compositionally controlled plasmonics in amorphous semiconductor metasurfaces. Opt Express *26*, 20861–20867.
80. Alquliah, A., Elkabbash, M., Cheng, J., Verma, G., Saraj, C.S., Li, W., and Guo, C. (2021). Reconfigurable metasurface-based 1 x 2 waveguide switch. Photon. Res. *9*, 2104–2115.
81. Dong, W., Liu, H., Behera, J.K., Lu, L., Ng, R.J.H., Sreekanth, K.V., Zhou, X., Yang, J.K.W., and Simpson, R.E. (2019). Wide Bandgap Phase Change Material Tuned Visible Photonics. Adv. Funct. Mater. *29*, 1806181.
82. Fang, Z., Zheng, J., Saxena, A., Whitehead, J., Chen, Y., and Majumdar, A. (2021). Non-Volatile Reconfigurable Integrated Photonics Enabled by Broadband Low-Loss Phase Change Material. Adv. Opt. Mater. *9*, 2002049.
83. Jia, W., Menon, R., and Sensale-Rodriguez, B. (2022). Visible and near-infrared programmable multi-level diffractive lenses with phase change material Sb2S3. Opt Express *30*, 6808–6817.
84. Meng, Q., Chen, X., Xu, W., Zhu, Z., Yuan, X., and Zhang, J. (2021). High Q Resonant Sb2S3-Lithium Niobate Metasurface for Active Nanophotonics. Nanomaterials *11*, 2373.
85. Sreekanth, K.V., Das, C.M., Medwal, R., Mishra, M., Ouyang, Q., Rawat, R.S., Yong, K.-T., and Singh, R. (2021a). Electrically Tunable Singular Phase and Goos–Hänchen Shifts in Phase-Change-Material-Based Thin-Film Coatings as Optical Absorbers. Adv. Mater. *33*, 2006926.
86. Sreekanth, K.V., Dong, W., Ouyang, Q., Sreejith, S., ElKabbash, M., Lim, C.T., Strangi, G., Yong, K.-T., Simpson, R.E., and Singh, R. (2018a). Large-Area Silver–Stibnite Nanoporous Plasmonic Films for Label-Free Biosensing. ACS Appl. Mater. Interfaces *10*, 34991–34999.
87. Sreekanth, K.V., ElKabbash, M., Caligiuri, V., Singh, R., De Luca, A., and Strangi, G. (2019a). New Directions in Thin Film Nanophotonics (Springer).
88. Sreekanth, K.V., Han, S., and Singh, R. (2018b). Ge2Sb2Te5-Based Tunable Perfect Absorber Cavity with Phase Singularity at Visible Frequencies. Adv. Mater. *30*, 1706696.
89. Sreekanth, K.V., Mahalakshmi, P., Han, S., Mani Rajan, M.S., Choudhury, P.K., and Singh, R. (2019b). Brewster Mode-Enhanced Sensing with Hyperbolic Metamaterial. Adv. Opt. Mater. *7*, 1900680.
90. Sreekanth, K.V., Medwal, R., Das, C.M., Gupta, M., Mishra, M., Yong, K.-T., Rawat, R.S., and Singh, R. (2021b). Electrically Tunable All-PCM Visible Plasmonics. Nano Lett. *21*, 4044–4050.
91. Sreekanth, K.V., Medwal, R., Srivastava, Y.K., Manjappa, M., Rawat, R.S., and Singh, R. (2021c). Dynamic Color Generation with Electrically Tunable Thin Film Optical Coatings. Nano Lett. *21*, 10070–10075.
92. Sreekanth, K.V., Ouyang, Q., Sreejith, S., Zeng, S., Lishu, W., Ilker, E., Dong, W., ElKabbash, M., Ting, Y., Lim, C.T., et al. (2019c). Phase-Change-Material-Based Low-Loss Visible-Frequency Hyperbolic Metamaterials for Ultrasensitive Label-Free Biosensing. Adv. Opt. Mater. *7*, 1900081.
93. Sreekanth, K.V., Prabhathan, P., Chaturvedi, A., Lekina, Y., Han, S., Zexiang, S., Tong Teo, E.H., Teng, J., and Singh, R. (2022). Wide-Angle Tunable Critical Coupling in Nanophotonic Optical Coatings with Low-Loss Phase Change Material. Small *18*, 2202005.
94. Yu, Y.F., Zhu, A.Y., Paniagua-Domínguez, R., Fu, Y.H., Luk'yanchuk, B., and Kuznetsov, A.I. (2015). High-transmission dielectric metasurface with 2π phase control at visible wavelengths. Laser Photon. Rev. *9*, 412–418.
95. Wang, M., Lee, J.S., Aggarwal, S., Farmakidis, N., He, Y., Cheng, T., and Bhaskaran, H. (2023). Varifocal Metalens Using Tunable and Ultralow-loss Dielectrics. Adv. Sci. *10*, 2204899.
96. Zhou, T., Gao, Y., Wang, G., Chen, Y., Gu, C., Bai, G., Shi, Y., and Shen, X. (2022). Reconfigurable hybrid silicon waveguide Bragg filter using ultralow-loss phase-change material. Appl. Opt. *61*, 1660–1667.
97. Ramer, R., and Chan, K.Y. (2022). Developing PCM-Based Microwave and Millimetre-Wave Switching Networks by Optimised Building Blocks. Electronics *11*, 3683. https://doi.org/10.3390/electronics11223683.
98. Kang, L., Jenkins, R.P., and Werner, D.H. (2019). Recent Progress in Active Optical Metasurfaces. Adv. Opt. Mater. *7*, 1801813.
99. Beruete, M., and Jáuregui-López, I. (2020). Terahertz Sensing Based on Metasurfaces. Adv. Opt. Mater. *8*, 1900721.
100. Yang, G., Zhao, L., Shen, C., Mao, Z., Xu, H., Feng, X., Wang, B., and Sui, X. (2020a). Boron nitride microsheets bridged with reduced graphene oxide as scaffolds for multifunctional shape stabilized phase change materials. Sol. Energy Mater. Sol. Cell. *209*, 110441.
101. Yang, H., Boulet, P., and Record, M.C. (2020b). Thermoelectric Properties of Sb-S System Compounds from DFT Calculations. Materials *13*, 4707.
102. Yang, Y., Zhang, L., Guo, D., Zhang, L., Yu, H., Liu, Q., Su, X., Shao, M., Song, M., Zhang, Y., et al. (2020c). Terahertz topological photonics for on-chip communication. Front. Psychiatr. *11*, 446–451.
103. Pitchappa, P., Kumar, A., Prakash, S., Jani, H., Medwal, R., Mishra, M., Rawat, R.S., Venkatesan, T., Wang, N., and Singh, R. (2021). Volatile Ultrafast Switching at Multilevel Nonvolatile States of Phase Change Material for Active Flexible Terahertz Metadevices. Adv. Funct. Mater. *31*, 2100200.
104. Cao, T., Lian, M., Chen, X., Mao, L., Liu, K., Jia, J., Su, Y., Ren, H., Zhang, S., Xu, Y., et al. (2022a). Multi-cycle reconfigurable THz extraordinary optical transmission using chalcogenide metamaterials. Opto-Electronic Science *1*, 210010–210011.
105. Cao, Y., Zeng, Z., Huang, D., Chen, Y., Zhang, L., and Sheng, X. (2022b). Multifunctional phase change composites based on biomass/MXene-derived hybrid scaffolds for excellent electromagnetic interference shielding and superior solar/electro-thermal energy storage. Nano Res. *15*, 8524–8535.
106. Zhang, S., Chen, X., Liu, K., Li, H., Xu, Y., Jiang, X., Xu, Y., Wang, Q., Cao, T., and Tian, Z. (2022a). Nonvolatile reconfigurable dynamic Janus metasurfaces in the terahertz regime. Photon. Res. *10*, 1731–1743.
107. Zhang, S., Chen, X., Liu, K., Li, H., Xu, Y., Jiang, X., Xu, Y., Wang, Q., Cao, T., and Tian, Z. (2022b). Nonvolatile reconfigurable terahertz wave modulator. PhotoniX *3*, 7.
108. Devi, K.M., Jana, A., Rane, S., Roy Choudhury, P., and Roy Chowdhury, D. (2022). Temperature tunable electromagnetically induced transparency in terahertz metasurface fabricated on ferroelectric platform. J. Phys. D Appl. Phys. *55*, 495103.
109. Lu, H., Thelander, E., Gerlach, J.W., Decker, U., Zhu, B., and Rauschenbach, B. (2013). Single Pulse Laser-Induced Phase Transitions of PLD-Deposited Ge2Sb2Te5 Films. Adv. Funct. Mater. *23*, 3621–3627.
110. Abdollahramezani, S., Hemmatyar, O., Taghinejad, H., Krasnok, A., Kiarashinejad, Y., Zandehshahvar, M., Alù, A., and Adibi, A. (2020). Tunable nanophotonics enabled by chalcogenide phase-change materials. Nanophotonics *9*, 1189–1241.
111. Wuttig, M., Bhaskaran, H., and Taubner, T. (2017). Phase-change materials for non-volatile photonic applications. Nat. Photonics *11*, 465–476.
112. Fang, Z., Chen, R., Zheng, J., Khan, A.I., Neilson, K.M., Geiger, S.J., Callahan, D.M.,

Moebius, M.G., Saxena, A., Chen, M.E., et al. (2022a). Ultra-low-energy programmable non-volatile silicon photonics based on phase-change materials with graphene heaters. Nat. Nanotechnol. *17*, 842–848.

113. Fang, Z., Chen, R., Zheng, J., and Majumdar, A. (2022b). Non-Volatile Reconfigurable Silicon Photonics Based on Phase-Change Materials. IEEE J. Sel. Top. Quant. Electron. *28*, 1–17.
114. Feldmann, J., Youngblood, N., Karpov, M., Gehring, H., Li, X., Stappers, M., Le Gallo, M., Fu, X., Lukashchuk, A., Raja, A.S., et al. (2021). Parallel convolutional processing using an integrated photonic tensor core. Nature *589*, 52–58.
115. Simpson, R.E., Yang, J.K.W., and Hu, J. (2022). Are phase change materials ideal for programmable photonics?: opinion. Opt. Mater. Express *12*, 2368–2373.
116. Zheng, J., Fang, Z., Wu, C., Zhu, S., Xu, P., Doylend, J.K., Deshmukh, S., Pop, E., Dunham, S., Li, M., and Majumdar, A. (2020). Nonvolatile Electrically Reconfigurable Integrated Photonic Switch Enabled by a Silicon PIN Diode Heater. Adv. Mater. *32*, 2001218.
117. Ríos, C., Du, Q., Zhang, Y., Popescu, C.-C., Shalaginov, M.Y., Miller, P., Roberts, C., Kang, M., Richardson, K.A., Gu, T., et al. (2021a). Ultra-compact nonvolatile photonics based on electrically reprogrammable transparent phase change materials. Preprint at arXiv. https://doi.org/10.48550/arXiv.2105.06010.
118. Ríos, C., Zhang, Y., Shalaginov, M.Y., Deckoff-Jones, S., Wang, H., An, S., Zhang, H., Kang, M., Richardson, K.A., Roberts, C., et al. (2021b). Multi-Level Electro-Thermal Switching of Optical Phase-Change Materials Using Graphene. Advanced Photonics Research *2*, 2000034.
119. Jeong-Sun, M., Hwa-Chang, S., Son, K.K., Eilam, Y., Kangmu, L., Elias, F., Geovanni, C., and Eric, P. (2019). Reconfigurable infrared spectral imaging with phase change materials. Proc. SPIE.
120. Martin-Monier, L., Popescu, C.C., Ranno, L., Mills, B., Geiger, S., Callahan, D., Moebius, M., and Hu, J. (2022). Endurance of chalcogenide optical phase change materials: a review. Opt. Mater. Express *12*, 2145–2167.
121. Gutiérrez, Y., Ovvyan, A.P., Santos, G., Juan, D., Rosales, S.A., Junquera, J., García-Fernández, P., Dicorato, S., Giangregorio, M.M., Dilonardo, E., et al. (2022). Interlaboratory study on Sb2S3 interplay between structure, dielectric function, and amorphous-to-crystalline phase change for photonics. iScience *25*, 104377.
122. Cui, Z., Bu, K., Zhuang, Y., Donnelly, M.-E., Zhang, D., Dalladay-Simpson, P., Howie, R.T., Zhang, J., Lü, X., and Hu, Q. (2021). Phase transition mechanism and bandgap engineering of Sb2S3 at gigapascal pressures. Commun. Chem. *4*, 125.
123. Guo, P., Sarangan, A., and Agha, I. (2019). A Review of Germanium-Antimony-Telluride Phase Change Materials for Non-Volatile Memories and Optical Modulators. Appl. Sci. *9*, 530.
124. Kondrotas, R., Chen, C., and Tang, J. (2018). Sb2S3 Solar Cells. Joule *2*, 857–878.
125. Faneca, J., Zeimpekis, I., Ilie, S.T., Bucio, T.D., Grabska, K., Hewak, D.W., and Gardes, F.Y. (2021). Towards low loss non-volatile phase change materials in mid index waveguides. Neuromorph. Comput. Eng. *1*, 014004.
126. Chamoli, S.K., Verma, G., Singh, S.C., and Guo, C. (2021). Phase change material based hot electron photodetection. Nanoscale *13*, 1311–1317.
127. Teo, T.Y., Krbal, M., Mistrik, J., Prikryl, J., Lu, L., and Simpson, R.E. (2022). Comparison and analysis of phase change materials-based reconfigurable silicon photonic directional couplers. Opt. Mater. Express *12*, 606–621.
128. Gao, K., Du, K., Tian, S., Wang, H., Zhang, L., Guo, Y., Luo, B., Zhang, W., and Mei, T. (2021). Intermediate Phase-Change States with Improved Cycling Durability of Sb2S3 by Femtosecond Multi-Pulse Laser Irradiation. Adv. Funct. Mater. *31*, 2103327.
129. Ovvyan, A.P., Gruhler, N., Ferrari, S., and Pernice, W.H.P. (2016). Cascaded Mach–Zehnder interferometer tunable filters. J. Opt. *18*, 064011.
130. Lu, L., Reniers, S.F.G., Wang, Y., Jiao, Y., and Simpson, R.E. (2022). Reconfigurable InP waveguide components using the Sb2S3 phase change material. J. Opt. *24*, 094001.
131. Ning, J., Wang, Y., Teo, T.Y., Huang, C.-C., Zeimpekis, I., Morgan, K., Teo, S.L., Hewak, D.W., Bosman, M., and Simpson, R.E. (2022). Low energy switching of phase change materials using a 2D thermal boundary layer. Preprint at arXiv. https://doi.org/10.48550/arXiv.2202.04699.
132. Thomson, D., Zilkie, A., Bowers, J.E., Komljenovic, T., Reed, G.T., Vivien, L., Marris-Morini, D., Cassan, E., Virot, L., Fédéli, J.M., et al. (2016). Roadmap on silicon photonics. J. Opt. *18*, 073003.
133. Shen, Y., Harris, N.C., Skirlo, S., Prabhu, M., Baehr-Jones, T., Hochberg, M., Sun, X., Zhao, S., Larochelle, H., Englund, D., and Soljačić, M. (2017). Deep learning with coherent nanophotonic circuits. Nat. Photonics *11*, 441–446.
134. Arrazola, J.M., Bergholm, V., Brádler, K., Bromley, T.R., Collins, M.J., Dhand, I., Fumagalli, A., Gerrits, T., Goussev, A., Helt, L.G., et al. (2021). Quantum circuits with many photons on a programmable nanophotonic chip. Nature *591*, 54–60.
135. Rogers, C., Piggott, A.Y., Thomson, D.J., Wiser, R.F., Opris, I.E., Fortune, S.A., Compston, A.J., Gondarenko, A., Meng, F., Chen, X., et al. (2021). A universal 3D imaging sensor on a silicon photonics platform. Nature *590*, 256–261.
136. Reed, G.T., Mashanovich, G., Gardes, F.Y., and Thomson, D.J. (2010). Silicon optical modulators. Nat. Photonics *4*, 518–526.
137. Alloatti, L., Palmer, R., Diebold, S., Pahl, K.P., Chen, B., Dinu, R., Fournier, M., Fedeli, J.-M., Zwick, T., Freude, W., et al. (2014). 100 GHz silicon–organic hybrid modulator. Light Sci. Appl. *3*, e173.
138. He, M., Xu, M., Ren, Y., Jian, J., Ruan, Z., Xu, Y., Gao, S., Sun, S., Wen, X., Zhou, L., et al. (2019a). High-performance hybrid silicon and lithium niobate Mach–Zehnder modulators for 100 Gbit s−1 and beyond. Nat. Photonics *13*, 359–364.
139. He, Q., Sun, S., and Zhou, L. (2019b). Tunable/Reconfigurable Metasurfaces: Physics and Applications. Research *2019*, 1849272.
140. Errando-Herranz, C., Takabayashi, A.Y., Edinger, P., Sattari, H., Gylfason, K.B., and Quack, N. (2020). MEMS for Photonic Integrated Circuits. IEEE J. Sel. Top. Quant. Electron. *26*, 1–16.
141. Wuttig, M., and Yamada, N. (2007). Phase-change materials for rewriteable data storage. Nat. Mater. *6*, 824–832.
142. Rudé, M., Pello, J., Simpson, R.E., Osmond, J., Roelkens, G., van der Tol, J.J.G.M., and Pruneri, V. (2013). Optical switching at 1.55 μm in silicon racetrack resonators using phase change materials. Appl. Phys. Lett. *103*, 141119.
143. Wu, C., Liu, X., Wu, X., Dong, F., Xu, J., and Zheng, Y. (2019). Low-Loss Integrated Photonic Switch Using Subwavelength Patterned Phase Change Material. ACS Photonics *658*, 87–94.
144. Xu, P., Zheng, J., Doylend, J.K., and Majumdar, A. (2019). Low-Loss and Broadband Nonvolatile Phase-Change Directional Coupler Switches. ACS Photonics *6*, 553–557.
145. Delaney, M., Zeimpekis, I., Du, H., Yan, X., Banakar, M., Thomson, D.J., Hewak, D.W., and Muskens, O.L. (2021). Nonvolatile programmable silicon photonics using an ultralow-loss Sb2Se3 phase change material. Sci. Adv. *7*, eabg3500.
146. Kato, K., Kuwahara, M., Kawashima, H., Tsuruoka, T., and Tsuda, H. (2017). Current-driven phase-change optical gate switch using indium–tin-oxide heater. APEX *10*, 072201.
147. Taghinejad, H., Abdollahramezani, S., Eftekhar, A.A., Fan, T., Hosseinnia, A.H., Hemmatyar, O., Eshaghian Dorche, A., Gallmon, A., and Adibi, A. (2021). ITO-based microheaters for reversible multi-stage switching of phase-change materials: towards miniaturized beyond-binary reconfigurable integrated photonics. Opt Express *29*, 20449–20462.
148. Meng, J., Gui, Y., Nouri, B.M., Comanescu, G., Ma, X., Zhang, Y., Popescu, C.-C., Kang, M., Miscuglio, M., Peserico, N., et al. (2022a). Electrical Programmable Low-loss high cyclable Nonvolatile Photonic Random-Access Memory. Preprint at arXiv13337. https://doi.org/10.48550/arxiv.2203.13337.
149. Meng, J., Gui, Y., Nouri, B.M., Comanescu, G., Ma, X., Zhang, Y., Popescu, C.-C., Kang, M., Miscuglio, M., Peserico, N., et al. (2022b). Electrical Programmable Multi-Level Non-volatile Photonic Random-Access Memory.
150. Meng, J., Peserico, N., Ma, X., Zhang, Y., Popescu, C.-C., Kang, M., Miscuglio, M., Richardson, K., Hu, J., and Sorger, V. (2022c). Electrical Programmable Low-Loss High Cyclable Nonvolatile Photonic Random-Access Memory.
151. Li, X., Youngblood, N., Ríos, C., Cheng, Z., Wright, C.D., Pernice, W.H., and Bhaskaran, H. (2019). Fast and reliable storage using a 5 bit, nonvolatile photonic memory cell. Optica *6*, 1–6.
152. Burr, G.W., Breitwisch, M.J., Franceschini, M., Garetto, D., Gopalakrishnan, K., Jackson, B., Kurdi, B., Lam, C., Lastras, L.A., Padilla, A., et al. (2010). Phase change memory technology. J. Vac. Sci. Technol. B *28*, 223–262.
153. Schuler, S., Muench, J.E., Ruocco, A., Balci, O., Thourhout, D.v., Sorianello, V., Romagnoli, M., Watanabe, K., Taniguchi, T., Goykhman, I., et al. (2021). High-responsivity graphene photodetectors integrated on silicon microring resonators. Nat. Commun. *12*, 3733.
154. Wang, L., Meric, I., Huang, P.Y., Gao, Q., Gao, Y., Tran, H., Taniguchi, T., Watanabe, K., Campos, L.M., Muller, D.A., et al. (2013).

One-Dimensional Electrical Contact to a Two-Dimensional Material. Science *342*, 614–617.
155. Eggleton, B.J., Luther-Davies, B., and Richardson, K. (2011). Chalcogenide photonics. Nat. Photonics *5*, 141–148.
156. Merklein, M., Kabakova, I.V., Büttner, T.F.S., Choi, D.-Y., Luther-Davies, B., Madden, S.J., and Eggleton, B.J. (2015). Enhancing and inhibiting stimulated Brillouin scattering in photonic integrated circuits. Nat. Commun. *6*, 6396.
157. Gan, S.X., Lai, C.K., Chong, W.Y., Choi, D.Y., Madden, S., and Ahmad, H. (2021). Optical phase transition of Ge2Sb2Se4Te1 thin film using low absorption wavelength in the 1550 nm window. Opt. Mater. *120*, 111450.
158. Pant, R., Poulton, C.G., Choi, D.-Y., McFarlane, H., Hile, S., Li, E., Thevenaz, L., Luther-Davies, B., Madden, S.J., and Eggleton, B.J. (2011). On-chip stimulated Brillouin scattering. Opt Express *19*, 8285–8290.
159. Merklein, M., Kabakova, I.V., Zarifi, A., and Eggleton, B.J. (2022). 100 years of Brillouin scattering: Historical and future perspectives. Appl. Phys. Rev. *9*, 041306.
160. Gan, S.X., Ng, K.B., Chew, J.W., Tey, L.S., Chong, W.S., Chong, W.Y., Goh, B.T., Lai, C.K., Madden, S., Choi, D.-Y., and Ahmad, H. (2022). Graphene oxide enhanced phase change tolerance of Ge2Sb2Se4Te1 for all-optical multilevel non-volatile photonics memory. J. Opt. Soc. Am. B *39*, 3004–3011.
161. Morrison, B., Casas-Bedoya, A., Ren, G., Vu, K., Liu, Y., Zarifi, A., Nguyen, T.G., Choi, D.-Y., Marpaung, D., Madden, S.J., et al. (2017). Compact Brillouin devices through hybrid integration on silicon. Optica *4*, 847–854.
162. Lai, C.K., Choi, D.-Y., Athanasios, N.J., Yan, K., Chong, W.Y., Debbarma, S., Ahmad, H., Eggleton, B.J., Merklein, M., and Madden, S.J. (2022). Hybrid Chalcogenide-Germanosilicate Waveguides for High Performance Stimulated Brillouin Scattering Applications. Adv. Funct. Mater. *32*, 2105230.
163. Eggleton, B.J., Poulton, C.G., Rakich, P.T., Steel, M.J., and Bahl, G. (2019). Brillouin integrated photonics. Nat. Photonics *13*, 664–677.
164. Sun, X., Zhang, L., Zhang, Q., and Zhang, W. (2019). Si Photonics for Practical LiDAR Solutions. Appl. Sci. *9*, 4225. https://doi.org/10.3390/app9204225.
165. Marpaung, D., Yao, J., and Capmany, J. (2019). Integrated microwave photonics. Nat. Photonics *13*, 80–90.
166. Garrett, M., Merklein, M., Liu, Y., Bui, C.T., Lai, C.K., Casas-Bedoya, A., Eggleton, B.J., Choi, D.Y., and Madden, S.J. (2022). Heterogeneous integration of Brillouin devices with active silicon photonic circuits. In 2022 IEEE Photonics Conference (IPC).
167. Smit, M., Leijtens, X., Ambrosius, H., Bente, E., van der Tol, J., Smalbrugge, B., de Vries, T., Geluk, E.-J., Bolk, J., van Veldhoven, R., et al. (2014). An introduction to InP-based generic integration technology. Semicond. Sci. Technol. *29*, 083001.
168. Yan, Z., Han, Y., Lin, L., Xue, Y., Ma, C., Ng, W.K., Wong, K.S., and Lau, K.M. (2021). A monolithic InP/SOI platform for integrated photonics. Light Sci. Appl. *10*, 200.
169. Zhu, D., Liu, Y., Gilbert, J.L., Cheng, R., Desiatov, B., Xin, C.J., Hu, Y., Holzgrafe, J., Ghosh, S., Shams-Ansari, A., et al. (2021). Integrated photonics on thin-film lithium niobate. Acta Biomater. *127*, 242–251.
170. Gholipour, B., Zhang, J., MacDonald, K.F., Hewak, D.W., and Zheludev, N.I. (2013). An All-Optical, Non-volatile, Bidirectional, Phase-Change Meta-Switch. Adv. Mater. *25*, 3050–3054.
171. Stern, L., Grajower, M., and Levy, U. (2014). Fano resonances and all-optical switching in a resonantly coupled plasmonic–atomic system. Nat. Commun. *5*, 4865.
172. Akola, J., and Jones, R.O. (2007). Structural phase transitions on the nanoscale: The crucial pattern in the phase-change materials Ge2Sb2Te5 and GeTe. Phys. Rev. B *76*, 235201.
173. Feinleib, J., Iwasa, S., Moss, S.C., deNeufville, J.P., and Ovshinsky, S.R. (1972). Reversible optical effects in amorphous semiconductors. J. Non-Cryst. Solids *8–10*, 909–916.
174. He, Q., Youngblood, N., Cheng, Z., Miao, X., and Bhaskaran, H. (2020). Dynamically tunable transmissive color filters using ultra-thin phase change materials. Opt Express *28*, 39841–39849.
175. Kohara, S., Kato, K., Kimura, S., Tanaka, H., Usuki, T., Suzuya, K., Tanaka, H., Moritomo, Y., Matsunaga, T., Yamada, N., et al. (2006). Structural basis for the fast phase change of Ge2Sb2Te5: Ring statistics analogy between the crystal and amorphous states. Appl. Phys. Lett. *89*, 201910.
176. Ahmadivand, A., Gerislioglu, B., Sinha, R., Karabiyik, M., and Pala, N. (2017). Optical Switching Using Transition from Dipolar to Charge Transfer Plasmon Modes in Ge2Sb2Te5 Bridged Metallodielectric Dimers. Sci. Rep. *7*, 42807.
177. Kumar, K., Duan, H., Hegde, R.S., Koh, S.C.W., Wei, J.N., and Yang, J.K.W. (2012). Printing colour at the optical diffraction limit. Nat. Nanotechnol. *7*, 557–561.
178. Shu, M.J., Zalden, P., Chen, F., Weems, B., Chatzakis, I., Xiong, F., Jeyasingh, R., Hoffmann, M.C., Pop, E., Philip Wong, H.S., et al. (2014). Ultrafast terahertz-induced response of GeSbTe phase-change materials. Appl. Phys. Lett. *104*, 251907.
179. Tian, X., and Li, Z.-Y. (2016). Visible-near infrared ultra-broadband polarization-independent metamaterial perfect absorber involving phase-change materials. Photon. Res. *4*, 146–152.
180. Tittl, A., Michel, A.-K.U., Schäferling, M., Yin, X., Gholipour, B., Cui, L., Wuttig, M., Taubner, T., Neubrech, F., and Giessen, H. (2015). A Switchable Mid-Infrared Plasmonic Perfect Absorber with Multispectral Thermal Imaging Capability. Adv. Mater. *27*, 4597–4603.
181. Kuznetsov, A.I., Miroshnichenko, A.E., Brongersma, M.L., Kivshar, Y.S., and Luk'yanchuk, B. (2016). Optically resonant dielectric nanostructures. Science *354*, aag2472.
182. Nikolaenko, A.E., De Angelis, F., Boden, S.A., Papasimakis, N., Ashburn, P., Di Fabrizio, E., and Zheludev, N.I. (2010). Carbon Nanotubes in a Photonic Metamaterial. Phys. Rev. Lett. *104*, 153902.
183. Wang, D., Zhang, L., Gu, Y., Mehmood, M.Q., Gong, Y., Srivastava, A., Jian, L., Venkatesan, T., Qiu, C.-W., and Hong, M. (2015). Switchable Ultrathin Quarter-wave Plate in Terahertz Using Active Phase-change Metasurface. Sci. Rep. *5*, 15020.
184. Kim, W., BrightSky, M., Masuda, T., Sosa, N., Kim, S., Bruce, R., Carta, F., Fraczak, G., Cheng, H.Y., Ray, A., et al. (2016). ALD-based confined PCM with a metallic liner toward unlimited endurance. In 2016 IEEE International Electron Devices Meeting (IEDM).
185. Nardone, M., Simon, M., Karpov, I.V., and Karpov, V.G. (2012). Electrical conduction in chalcogenide glasses of phase change memory. J. Appl. Phys. *112*, 071101.
186. Cai, W., and Shalaev, V. (2009). Optical Metamaterials: Fundamentals and Applications (Springer).
187. Zhu, W.M., Liu, A.Q., Zhang, X.M., Tsai, D.P., Bourouina, T., Teng, J.H., Zhang, X.H., Guo, H.C., Tanoto, H., Mei, T., et al. (2011). Switchable Magnetic Metamaterials Using Micromachining Processes. Adv. Mater. *23*, 1792–1796.
188. Piccinotti, D., Gholipour, B., Yao, J., MacDonald, K.F., Hayden, B.E., and Zheludev, N.I. (2019). Stoichiometric Engineering of Chalcogenide Semiconductor Alloys for Nanophotonic Applications. Adv. Mater. *31*, 1807083.
189. Mandal, A., Cui, Y., McRae, L., and Gholipour, B. (2021). Reconfigurable chalcogenide phase change metamaterials: a material, device, and fabrication perspective. J. Phys. Photonics *3*, 022005.
190. Wang, Q., Rogers, E.T.F., Gholipour, B., Wang, C.-M., Yuan, G., Teng, J., and Zheludev, N.I. (2016). Optically reconfigurable metasurfaces and photonic devices based on phase change materials. Nat. Photonics *10*, 60–65.
191. Martins, T., Cui, Y., Gholipour, B., Ou, J.-Y., Frazão, O., and MacDonald, K.F. (2021). Fiber-Integrated Phase Change Metasurfaces with Switchable Group Delay Dispersion. Adv. Opt. Mater. *9*, 2100803.
192. Martins, T., Gholipour, B., Piccinotti, D., MacDonald, K.F., Peacock, A.C., Frazão, O., and Zheludev, N.I. (2019). Fiber-integrated phase-change reconfigurable optical attenuator. APL Photonics *4*, 111301.
193. Ding, K., Wang, J., Zhou, Y., Tian, H., Lu, L., Mazzarello, R., Jia, C., Zhang, W., Rao, F., and Ma, E. (2019). Phase-change heterostructure enables ultralow noise and drift for memory operation. Science *366*, 210–215.
194. Popescu, M. (2006). Chalcogenides – Past, present, future. J. Non-Cryst. Solids *37*, 887–891.
195. McRae, L., Xie, Y., and Gholipour, B. (2021). Photoionic Driven Movement of Metallic Ions as a Nonvolatile Reconfiguration Mechanism in Amorphous Chalcogenide Metasurfaces. Adv. Opt. Mater. *9*, 2101046.
196. Jia, W., Menon, R., and Sensale-Rodriguez, B. (2021). Unique prospects of phase change material Sb2Se3 for ultra-compact reconfigurable nanophotonic devices. Opt. Mater. Express *11*, 3007–3014.
197. Caño, I., Vidal-Fuentes, P., Calvo-Barrio, L., Alcobé, X., Asensi, J.M., Giraldo, S., Sánchez, Y., Jehl, Z., Placidi, M., Puigdollers, J., et al. (2022). Does Sb(2)Se(3) Admit Nonstoichiometric Conditions? How Modifying the Overall Se Content Affects the Structural, Optical, and Optoelectronic Properties of Sb(2)Se(3) Thin Films. ACS Appl. Mater. Interfaces *14*, 11222–11234.
198. Xie, Y., Kim, W., Kim, Y., Kim, S., Gonsalves, J., BrightSky, M., Lam, C., Zhu, Y., and Cha, J.J. (2018). Self-Healing of a Confined Phase Change Memory Device with a Metallic Surfactant Layer. Adv. Mater. *30*, 1705587.

199. Guo, Y.R., Dong, F., Qiao, C., Wang, J.J., Wang, S.Y., Xu, M., Zheng, Y.X., Zhang, R.J., Chen, L.Y., Wang, C.Z., and Ho, K.M. (2018). Structural signature and transition dynamics of Sb2Te3 melt upon fast cooling. Phys. Chem. Chem. Phys. *20*, 11768–11775.
200. Aftab, W., Huang, X., Wu, W., Liang, Z., Mahmood, A., and Zou, R. (2018). Nanoconfined phase change materials for thermal energy applications. Energy Environ. Sci. *11*, 1392–1424.
201. Aftab, W., Usman, A., Shi, J., Yuan, K., Qin, M., and Zou, R. (2021). Phase change material-integrated latent heat storage systems for sustainable energy solutions. Energy Environ. Sci. *14*, 4268–4291.
202. Chen, X., Cheng, P., Tang, Z., Xu, X., Gao, H., and Wang, G. (2021). Carbon-based composite phase change materials for thermal energy storage, transfer, and conversion. Adv. Sci. *8*, 2001274.
203. Chen, X., Tang, Z., Gao, H., Chen, S., and Wang, G. (2020b). Phase change materials for electro-thermal conversion and storage: from fundamental understanding to engineering design. iScience *23*, 101208.
204. Chen, X., Gao, H., Tang, Z., Dong, W., Li, A., and Wang, G. (2020a). Optimization strategies of composite phase change materials for thermal energy storage, transfer, conversion and utilization. Energy Environ. Sci. *13*, 4498–4535.
205. Li, T., Wu, M., Wu, S., Xiang, S., Xu, J., Chao, J., Yan, T., Deng, T., and Wang, R. (2021). Highly conductive phase change composites enabled by vertically-aligned reticulated graphite nanoplatelets for high-temperature solar photo/electro-thermal energy conversion, harvesting and storage. Nano Energy *89*, 106338.
206. Liu, Z., Zou, R., Lin, Z., Gui, X., Chen, R., Lin, J., Shang, Y., and Cao, A. (2013). Tailoring Carbon Nanotube Density for Modulating Electro-to-Heat Conversion in Phase Change Composites. Nano Lett. *13*, 4028–4035.
207. Li, A., Dong, C., Dong, W., Yuan, F., Gao, H., Chen, X., Chen, X.-B., and Wang, G. (2020). Network Structural CNTs Penetrate Porous Carbon Support for Phase-Change Materials with Enhanced Electro-Thermal Performance. Adv. Electron. Mater. *6*, 1901428.
208. Kou, Y., Sun, K., Luo, J., Zhou, F., Huang, H., Wu, Z.-S., and Shi, Q. (2021). An intrinsically flexible phase change film for wearable thermal managements. Energy Storage Mater. *34*, 508–514.
209. Li, G., Zhang, X., Wang, J., and Fang, J. (2016). From anisotropic graphene aerogels to electron- and photo-driven phase change composites. J. Mater. Chem. A Mater. *4*, 17042–17049.
210. Wei, X., Cho, K.S., Thee, E.F., Jager, M.J., Chen, D.F., Yuan, Y.-p., and Wang, Y. (2019). Photo- and electro-responsive phase change materials based on highly anisotropic microcrystalline cellulose/graphene nanoplatelet structure. J. Neurosci. Res. *97*, 70–76.
211. Xue, F., Jin, X.-z., Wang, W.-y., Qi, X.-d., Yang, J.-h., and Wang, Y. (2020). Melamine foam and cellulose nanofiber co-mediated assembly of graphene nanoplatelets to construct three-dimensional networks towards advanced phase change materials. Nanoscale *12*, 4005–4017.
212. Umair, M.M., Zhang, Y., Tehrim, A., Zhang, S., and Tang, B. (2020). Form-Stable Phase-Change Composites Supported by a Biomass-Derived Carbon Scaffold with Multiple Energy Conversion Abilities. Ind. Eng. Chem. Res. *59*, 1393–1401.
213. Xiao, Y.-y., Bai, D.-y., Xie, Z.-p., Yang, Z.-y., Yang, J.-h., Qi, X.-d., and Wang, Y. (2021). Flexible copper foam-based phase change materials with good stiffness-toughness balance, electro-to-thermal conversion ability and shape memory function for intelligent thermal management. Compos. Appl. Sci. Manuf. *146*, 106420.
214. Shahid, U.B., and Abdala, A. (2021). A critical review of phase change material composite performance through Figure-of-Merit analysis: Graphene vs Boron Nitride. Energy Storage Mater. *34*, 365–387.
215. Cheng, P., Tang, Z., Gao, Y., Liu, P., Liu, C., and Chen, X. (2022). Flexible engineering of advanced phase change materials. iScience *25*, 104226.
216. Xue, F., Qi, X.-d., Huang, T., Tang, C.-y., Zhang, N., and Wang, Y. (2021). Preparation and application of three-dimensional filler network towards organic phase change materials with high performance and multi-functions. Chem. Eng. J. *419*, 129620.
217. Yang, J., Li, J., He, S., Wang, L.V., Liu, Z.-Y., Xie, B.-H., Yang, M.-B., and Yang, W. (2019). High-performance composite phase change materials for energy conversion based on macroscopically three-dimensional structural materials. Optica *6*, 250–256.
218. Wu, S., Song, Y., Chen, S., Zheng, M., Ma, Y., Cui, L., and Jonas, J.B. (2020). Thermal conductivity enhancement on phase change materials for thermal energy storage: A review. Energy Storage Mater. *76*, 251–258.
219. Li, G., Hong, G., Dong, D., Song, W., and Zhang, X. (2018). Multiresponsive Graphene-Aerogel-Directed Phase-Change Smart Fibers. Adv. Mater. *30*, 1801754.

Update

iScience
Volume 26, Issue 12, 15 December 2023, Page

DOI: https://doi.org/10.1016/j.isci.2023.108396

iScience

CellPress
OPEN ACCESS

Correction

Roadmap for phase change materials in photonics and beyond

Patinharekandy Prabhathan, Kandammathe Valiyaveedu Sreekanth, Jinghua Teng, Joo Hwan Ko, Young Jin Yoo, Hyeon-Ho Jeong, Yubin Lee, Shoujun Zhang, Tun Cao, Cosmin-Constantin Popescu, Brian Mills, Tian Gu, Zhuoran Fang, Rui Chen, Hao Tong, Yi Wang, Qiang He, Yitao Lu, Zhiyuan Liu, Han Yu, Avik Mandal, Yihao Cui, Abbas Sheikh Ansari, Viraj Bhingardive, Myungkoo Kang, Choon Kong Lai, Moritz Merklein, Maximilian J. Müller, Young Min Song, Zhen Tian, Juejun Hu, Maria Losurdo, Arka Majumdar, Xiangshui Miao, Xiao Chen, Behrad Gholipour, Kathleen A. Richardson, Benjamin J. Eggleton, Kanudha Sharda,* Matthias Wuttig,* and Ranjan Singh*

(iScience *26*, 107946; October 20, 2023)

In the original published version of this article, the list of authors included the in-house *iScience* editor who helped coordinate the writing, Dr. Kanudha Sharda. Elsevier's conflict of interest policy (https://www.cell.com/iscience/authors#policies) is prescriptive of cases in which full-time editors can be authors of papers published in Elsevier's journals. This case fell outside of policy, and Dr. Sharda should not have been included in the author list. We have corrected the original article online to remove the editor's name and edited the declaration of interest to reflect this change. All authors have been informed prior to this change. The editorial office apologizes for this oversight.

*Correspondence: k.sharda@cell.com (K.S.), wuttig@physik.rwth-aachen.de (M.W.), ranjans@ntu.edu.sg (R.S.)
https://doi.org/10.1016/j.isci.2023.108396